**Effect of Well Pattern to the Water Alternating Gas (WAG) Carbon Dioxide Injection on Angsi I-35 Reservoir**

by

Ahmad Ehsan bin Ahmad Ruslan

Dissertation submitted in partial fulfilment of

the requirements for the

Bachelor of Engineering (Hons)

(Mechanical Engineering)

JULY 2008

Universiti Teknologi PETRONAS
Bandar Seri Iskandar
31750 Tronoh
Perak Darul Ridzuan

CERTIFICATION OF APPROVAL

**Effect of Well Pattern to the Water Alternating Gas (WAG) Carbon Dioxide Injection on Angsi I-35 Reservoir**

by

Ahmad Ehsan bin Ahmad Ruslan

A project dissertation submitted to the

Mechanical Engineering Programme

Universiti Teknologi PETRONAS

in partial fulfilment of the requirement for the

BACHELOR OF ENGINEERING (Hons)

(MECHANICAL ENGINEERING)

Approved by,

_____

(Pn Faiza Mohamed Nasir)
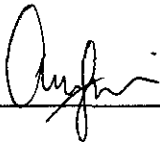
UNIVERSITI TEKNOLOGI PETRONAS

TRONOH, PERAK

July 2008

# CERTIFICATION OF ORIGINALITY

This is to certify that I am responsible for the work submitted in this project, that the original work is my own except as specified in the references and acknowledgements, and that the original work contained herein have not been undertaken or done by unspecified sources or persons.


AHMAD EHSAN BIN AHMAD RUSLAN

# ABSTRACT

This work presents the effect of different well pattern on the Water-alternating-gas (WAG) carbon dioxide injection for Angsi I-35 reservoir in offshore Terengganu. The use of WAG $CO_2$ injection seems to be the most promising option as enhanced oil recovery method for Angsi I-35 field. This work focuses on the five typical well patterns: five-spot, seven-spot, inverted seven-spot, direct line drive and staggered line drive. The prediction of oil recovery for each of the pattern was conducted using simple theoretical calculations, which are based on the sweep efficiency equation, and by using numerical simulations. The results obtained from both methods were compared in order to identify the well pattern that gives the highest recovery. It was found that inverted seven-spot pattern yields the highest oil recovery of 52%, which was about 12% more from the current recovery under natural production. The cost incurred by employing different well patterns was also analysed. The most profitable well pattern was the inverted seven-spot which gives the highest percentage of internal rate return (IRR) at 96.91% and the least profitable option was seven spot well patterns as it laid the lowest percentage of IRR at 53.79%. Cost analysis confirmed that all well patterns offered good results in term of profitability as all of them exceeded the minimum attractive IRR limit which is at 30%, hence proving that all the five well patterns are feasible to be conducted.

# ACKNOWLEDGEMENT

First and foremost, I would like to thank God the Almighty for the blessings upon completing my Final Year Project which is a partial fulfillment of the requirements for the Bachelor of Engineering (Hons) in Mechanical Engineering. A special gratitude to my respectable supervisor; Pn. Faiza binti Mohamed Nasir, who found her time in a very busy schedule to assist and guide me, monitored my progress and answered my inquiry. Her supervision and leadership has been great in directing me through the correct path towards completing this project. I am also deeply grateful for her guidance, encouragement and patience throughout the duration of the project.

My gratitude and appreciation also to Mr Muhammad Sanif Maulut who had guided me throughout my project by providing me with the technical knowledge of Eclipse100. I have very much benefited from his professional and personal advice. In this little moment I would also like to convey my appreciation towards Dr Sonny Irawan, Mr Elias bin Abllah, Dr Ismail Mohd Saaid and AP Dr Razali Hamzah who had guided me on how to improve the project during the seminar. Finally yet importantly, to all the people who have given their cooperation either directly or indirectly, thank you for being there for me, and for helping me, and most of all, for all the support during the period of my Final Year Project.

# TABLE OF CONTENTS

# APPENDICES

# LIST OF FIGURES

## LIST OF TABLES

# ABBREVIATIONS AND NOMENCLATURES

| | |
|---|---|
| WAG | water alternating gas |
| $CO_2$ | carbon dioxide |
| EOR | enhanced oil recovery |
| BPD | barrels per day |
| SCFD | standard cubic feet per day |
| LPG | liquefied petroleum gas |
| RF | recovery factor |
| SPE | society of petroleum engineers |
| FOE | field oil efficiency |
| OIP | oil in place |
| HCPV | hydrocarbon pore volume |
| FOPR | field oil production rate |
| UTC | unit technical cost |

# CHAPTER 1

# INTRODUCTION

Nowadays, secondary recovery methods are now introduced much earlier in the life of a field; often well before the end of the primary production phase. However, before undertaking a secondary recovery project it should be clearly proven that the natural recovery processes are insufficient; otherwise there is a risk that the heavy capital investment required may be completely wasted. A certain amount of production data is therefore required. Nonetheless, if a reservoir is produced too long during the primary phase the chances of successful secondary recovery phase may be reduced.

The efficiency of an enhanced recovery method is a measure of its ability to provide greater hydrocarbon recovery than by natural depletion, at an economically attractive production rate [1]. The efficiency of an enhanced recovery method depends on:

a) the reservoir characteristics

b) the nature of the displacing and displaced fluids

c) the arrangement of production and injection wells

the latter being the interest of the study for water alternating gas (WAG) carbon dioxide injection on Angsi I-35 reservoir field.

## 1.1 Problem Statement

$CO_2$ injection has been identified to be the most feasible enhanced oil recovery process for Malaysian field [1]. The performance of the injection is affected by the well spacing in a well pattern, where it is ideal to place the wells as closest as possible. However

there will be a huge cost impact. Therefore it is important to verify the optimum position and investigate the cost impact.

## 1.2 Significance of Study

Focus on WAG $CO_2$ injection is appropriate because $CO_2$ is the second most applied enhanced oil recovery (EOR) process in the world, behind steam flooding. In considering $CO_2$ feasibility, the most important flood variables to consider is the ability of the $CO_2$ to contact a large portion of the reservoir, including vertical, areal and unit displacement (all of which depend on well spacing, mobility ratio, permeability, reservoir heterogeneity and geometry, injection well conformance, areal discontinuity, gas cap, and fracture system).

## 1.3 Objectives

The main objective of the project is to provide an improved well pattern for carrying out secondary and tertiary recovery operations and to find the most optimum well spacing for Angsi I-35 field.

## 1.4 Scope of Works

The scope of work for this project includes:-

i. Conducting extensive literature review on water alternating gas (WAG) injection, on how well patterns with different spacing may affect the performance of the recovery method on Angsi I-35 reservoir

ii. Theoretical study of different well patterns and develop mathematical model to predict the recovery of each patterns in term of their sweep efficiencies.

iii. Justifying the mathematical model by executing simulation study using Eclipse 100

iv. As it is ideal to place the wells as closest as possible to optimize the performance of the injection, there will be a significance cost impact. Hence, it is essential to verify the best position and execute a simple cost analysis to investigate the cost impact.

# CHAPTER 2

# LITERATURE REVIEW

## 2.1 Angsi Field

Angsi field is located approximately 165 kilometres off the East Coast of Peninsular Malaysia in a water depth of 69 metres mean sea level. The Angsi-A Complex, comprising of a central processing platform, a drilling/riser platform and a 100-m long interconnecting bridge is the host and processing platform for AnDP-B, AnDP-C, AnDP-E, AnDP-D, future nearby platforms such as Besar as well as a southern hub for gas from PM-9 and future southern gas fields. Figure 2.1 below shows location map of the Angsi Field.
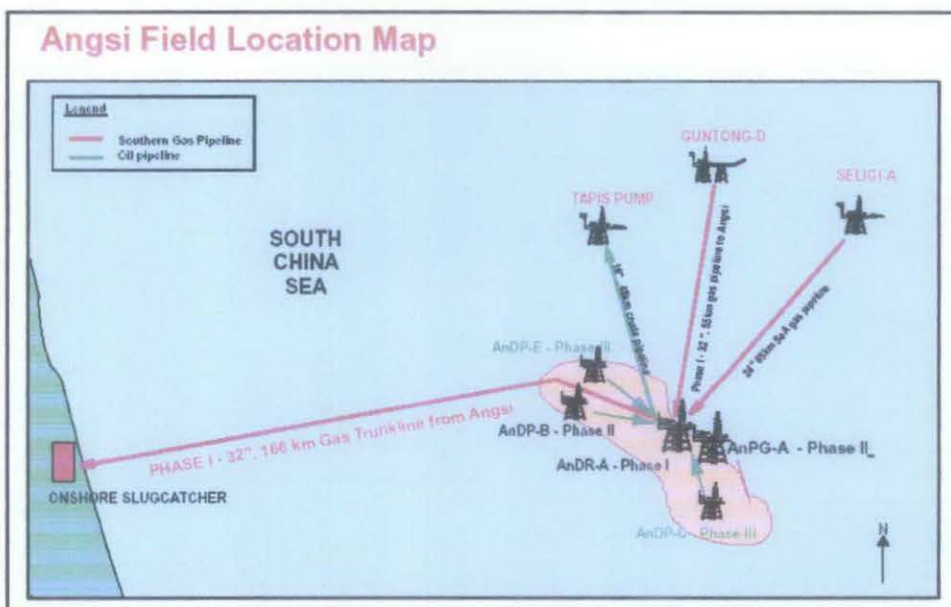


Figure 2.1: Angsi field location map [2]

The field began its oil production with an initial flow of 15,000 barrels per day (BPD), while its gas production started at about 60 million standard cubic feet per day (SCFD). At its peak, the field is expected to produce about 65,000 BPD of oil and 450 million SCFD of gas, which is equivalent to 10 per cent and 17 per cent respectively of the country's current total oil and gas production [2].

The development of Angsi is a key element in meeting Malaysia's burgeoning energy needs in the coming decades, with 160 million barrels of oil and 1.4 tcf of gas expected to be produced from the field. An additional Angsi development phase is currently under evaluation to further maximise resource recovery.

Angsi I-35 is one of the major oil bearing reservoirs reside in the Angsi field. It has a sizeable gas cap and consists of 11 layers. The reservoir is sloppy and wide in area. The properties of Angsi I-35 are tabulated on Table 2.1 below:

Table 2.1: Properties of Angsi I-35 reservoir

| Angsi I-35 reservoir properties | |
|---|---|
| Pressure | 3420psia |
| Water formation volume factor at reservoir pressure | 1.025 |
| Viscosity of water at reservoir pressure | 0.32cp |
| Oil API gravity | 42.2 |
| Water specific gravity | 1 |
| Gas specific gravity | 0.688 |
| Rock compressibility | 0.0000035 1/psi |
| Datum depth | 8075ft |
| Pressure at the datum depth | 4500psia |
| Depth of water-oil contact | 8900ft |

## 2.2 Miscible Displacement

Miscible displacement is a major branch of enhanced oil recovery processes. Miscible displacement is an injection processes that introduce miscible gases into the reservoir. A miscible displacement process maintains reservoir pressure and improves oil displacement because the interfacial tension between oil and water is reduced. Injected gases include liquefied petroleum gas (LPG), such as propane, methane under high pressure, methane enriched with light hydrocarbons, nitrogen under high pressure, and carbon dioxide ($CO_2$) under suitable reservoir conditions of temperature and pressure. The fluid most commonly used for miscible displacement is carbon dioxide due to availability and its ability to reduce the oil viscosity. $CO_2$ is less expensive than liquefied petroleum gas [3]. Figure 2.2 shows the schematic diagram of miscible $CO_2$ injection process.
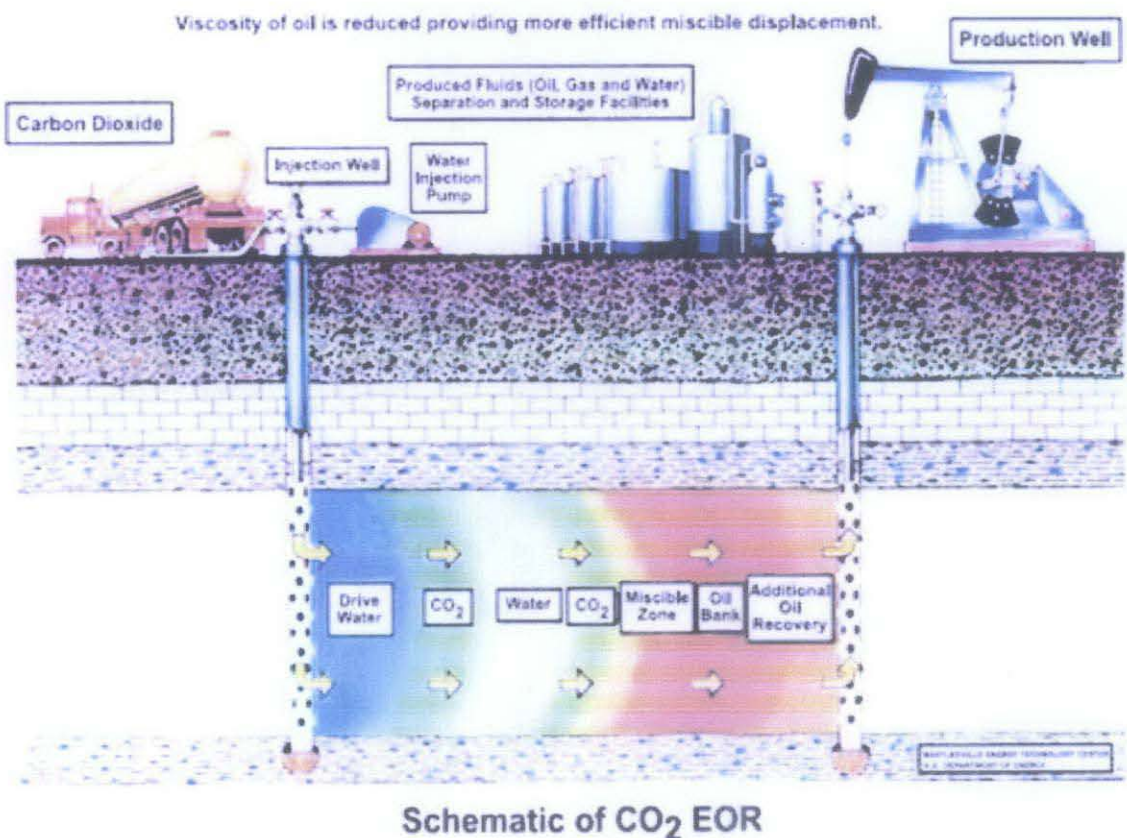
Figure 2.2: Schematic diagram of miscible displacement process [13]

The practical success of $CO_2$ injection depends on [4]:

    i.      the oil characteristics

    ii.     the part of the reservoir effectively contacted

    iii.    the attainable pressure

    iv.    the availability and cost of the $CO_2$

Carbon dioxide may be used as a gas, dissolved in water or in an alternating slug scheme. The very high solubility of carbon dioxide in oil and to a lesser extent in water results in [1]:

    i.      a large reduction in oil viscosity and a small increase in water viscosity. This results in a significant improvement of oil mobility in the reservoir

    ii.     swelling of the oil by 10 to 20%, depending on its type and saturation pressure

    iii.    a reduction in oil density. This lessens the effect of gravity segregation during the injection of gaseous carbon dioxide

    iv.    a lowering of the interfacial tension. With $CO_2$ in the gaseous state at high enough pressure, miscibility with oil may be achieved

    v.     chemical action on carbonate or shaly rocks

## 2.3 Combined Gas and Water Injection

In the conventional alternating $CO_2$ and water chased with water method, a predetermined slug of $CO_2$ is injected in cycles in which equal volumes of gas and water alternate at a constant gas/water ratio, or WAG ratio. After the total $CO_2$ slug volume has been injected, a chase of continuous water is started [1]. This injection design is most effective in highly stratified heterogeneous reservoirs because it minimizes gas cycling in high-velocity layers by reducing the fraction of injected $CO_2$ entering those layers. Accurate characterization of reservoir heterogeneity is extremely important for design of large $CO_2$ floods because the volumetric sweep resulting from reservoir heterogeneity dictates the $CO_2$ utilization factor (the amount of $CO_2$ required to recover the desired amount of oil).

7

The theory behind the combined gas and water injection process is by successfully injecting slugs of water and gas; a homogeneous mixture will be formed within the pores due to relative permeability effects. This mixture will behave as a fluid of low mobility. Thus, the mobility ratio of the system gas and water/oil will be reduced and the displacement efficiency improved. Alternate injection is preferred to simultaneous injection for the following reasons [1]:

a) higher injectivity

b) cheaper and simpler surface equipment

c) better vertical distribution of the two fluids throughout the thickness of the formation

## 2.4 Numerical Simulation of Miscible Flood Model

The black oil simulator utilizes miscible flood model which is an implementation of the empirical treatment suggested by M. Todd and W. Longstaff [5].The model is a 3-component system consisting of reservoir oil, injection gas solvent ($CO_2$) and water. The reservoir oil component consists of stock tank oil together with the associated solution gas. $CO_2$ and reservoir oil components are assumed to be miscible in all proportions and consequently only one hydrocarbon phase exists in the reservoir. The relative permeability requirements of the model are those for a two-phase system (water/hydrocarbon). The Todd-Longstaff [5] mixing parameter technique requires modification of the viscosity and density calculations in a black oil simulator.

The Todd-Longstaff [5] model is an empirical treatment of the effects of physical dispersion between the miscible components in the hydrocarbon phase. The model introduces an empirical parameter, $\omega$, whose value lies between 0 and 1, to represent the size of the dispersed zone in each grid cell. The value of $\omega$ thus controls the degree of fluid mixing within each grid cell. The mixing parameter model would be of limited use

unless the mixing parameter could itself be modeled over a wide range of operating conditions. A value of ω=1 models the case when the size of the dispersed zone is much greater than a typical grid cell size and the hydrocarbon components can be considered to be fully mixed in each cell. In this case the miscible components have the same value for the viscosity and density, as given by the appropriate mixing rule formulae resulting in a piston-like displacement of oil by the injected $CO_2$.

A value of ω=0 models the effect of a negligibly thin dispersed zone between the gas and oil components, and the miscible components should then have the viscosity and density values of the pure components. The displacement is similar to an immiscible displacement (except for the treatment of relative permeability).In practical applications an intermediate value of ω would be needed to model incomplete mixing of the miscible components. An intermediate value of ω results in a continuous solvent saturation increase behind the solvent front. Todd-Longstaff [5] accounted for the effects of viscous fingering effects in 2-D studies by setting ω=2/3 independent of mobility ratio, by that setting the empirical mixing parameter of Angsi I-35 equal to 0.667.

One of the features that have to be modeled for miscible gas injection processes is the screening effect of high water saturation on the contact between the miscible gas and the in-place oil in each grid cell. The effective residual oil saturation to a miscible gas drive is found to increase with increasing water saturation and correct modeling of the effect is important since it may reduce the efficiency of the miscible displacement. The process is modeled by introducing effective residual oil saturation, $S_{or}$ which depends on the water saturation ($S_{or} = S_{or}(S_w)$). Mobile oil saturation is then calculated by:

$$S_o^* = MAX(S_o - S_{or}, 0.0) \dots\dots\dots\dots\dots\dots\dots\dots\dots\dots\dots\dots\dots(2.1)$$

The mobile oil saturation, $S_o^*$ is then used to determine the relative permeabilities of miscible components and the effective gas and oil viscosities and densities in each grid cell.

9

## 2.4.1 Relative Permeability Model

$CO_2$ and reservoir oil are considered to be miscible components of the hydrocarbon (non-wetting) phase. The flow is two-phase in character and two-phase relative permeability curves need to be defined for the water and hydrocarbon phases, $k_{rw}(S_w)$ and $k_m(S_n)$ where:

$S_w$ = water saturation

$S_n = S_o + S_s$ = hydrocarbon phase saturation

$k_m$ = relative permeability of oil as measured in a water flood test

The oil and $CO_2$ relative permeabilites are proportional to their local volume ratio in the hydrocarbon phase:

$$k_{ro} = \frac{S_o}{S_o + S_s} k_m(S_n) \quad\text{.......................................(2.2)}$$

and

$$k_{rs} = \frac{S_s}{S_o + S_s} k_m(S_n) \quad\text{.......................................(2.3)}$$

Also, it is possible to modify the straight line miscible relative permeabilities by introducing function. In this case the oil and miscible gas relative permeabilities are:

$$k_{ro} = M_{kro} \frac{S_o}{S_o + S_s} k_m(S_n) \quad\text{.......................................(2.4)}$$

and

$$k_{rs} = M_{krs} \frac{S_s}{S_o + S_s} k_m(S_n) \quad\text{.......................................(2.5)}$$

where $M_{kro}$ and $M_{krs}$ are misicible relative permeabilities function.

## 2.4.2 Viscosity Model

The following form is suggested by Todd-Longstaff [5] for the effective oil and $CO_2$ viscosities to be used in an immiscible simulator:

$$\mu_{oeff} = \mu_o^{1-\omega} \mu_m^{\omega} \quad\text{.............................................................................(2.6)}$$

and

$$\mu_{seff} = \mu_s^{1-\omega} \mu_m^{\omega} \quad\text{..............................................................................(2.7)}$$

From the equation above, if $\omega = 1$ then $\mu_{o\,eff} = \mu_{s\,eff} = \mu_m$ where $\mu_m$ is the viscosity of a fully mixed oil-solvent system. The formula to be used for $\mu_m$ is the 1/4-power fluid mixing rule:

$$\frac{1^{1/4}}{\mu_m} = \frac{S_s}{S_n}\left(\frac{1}{\mu_s}\right)^{1/4} + \frac{S_s}{S_n}\left(\frac{1}{\mu_o}\right)^{1/4} \quad\text{.........................................................(2.8)}$$

$$\mu_m = \frac{\mu_o \mu_s}{\left(\dfrac{S_s}{S_n} \cdot \mu^{1/4} + \dfrac{S_o}{S_n} \cdot \mu_s^{1/4}\right)^4} \quad\text{.......................................................(2.9)}$$

The case $\omega=1$ models a large dispersed oil-solvent zone. The Todd-Longstaff [5] model treats this case as a local unit mobility ratio displacement. If $\omega=0$ then $\mu_{o\,eff} = \mu_o$ and $\mu_{s\,eff} = \mu_s$. Each component has an effective viscosity equal to its pure value. Such a case corresponds to a local high adverse mobility ratio displacement and models a negligibly thin oil-solvent dispersed zone. The mixing parameter approach allows the case of a partial mixing zone to be modeled by choosing an intermediate value of $\omega$.

### 2.4.3 Component Density Model

The treatment of effective oil and $CO_2$ densities is based on the same 1/4-power rule as the effective viscosities. By default the density calculation will use the same mixing parameter as the viscosity. However, a separate mixing parameter may optionally be specified for the effective density calculation.

The densities are computed by first, the partially mixed or effective viscosities are calculated using equations 2.6, equation 2.7, equation 2.8 an equation 2.9 above. The value of each effective component viscosity is then used in turn in equation 2.8 and

11

equation 2.9 to yield an effective saturation fraction to be used in oil and solvent density calculations. The effective saturation fractions used for density calculations are:

$$\left(\frac{S_o}{S_n}\right)_{oe} = \frac{\mu_{oeff}^{1/4} \cdot \mu_o^{1/4} - \mu_s^{1/4} \cdot \mu_o^{1/4}}{\mu_{oeff}^{1/4} \cdot \left(\mu_o^{1/4} - \mu_s^{1/4}\right)} \quad\text{.........................................(2.10)}$$

and

$$\left(\frac{S_o}{S_n}\right)_{se} = \frac{\mu_{seff}^{1/4} \cdot \mu_o^{1/4} - \mu_s^{1/4} \cdot \mu_o^{1/4}}{\mu_{seff}^{1/4} \cdot \left(\mu_o^{1/4} - \mu_s^{1/4}\right)} \quad\text{.........................................(2.11)}$$

The effective oil density ($\rho_{o\ eff}$) and $CO_2$ density ($\rho_{s\ eff}$) are now computed from the effective saturations fractions in equation 2.10 and equation 2.11 and the pure component densities ($\rho_o$, $\rho_s$) using the following formula:

$$\rho_{oeff} = \rho_o \left(\frac{S_o}{S_n}\right)_{oe} + \rho_s \left[1 - \left(\frac{S_o}{S_n}\right)_{oe}\right] \quad\text{.........................................(2.12)}$$

and

$$\rho_{seff} = \rho_o \left(\frac{S_o}{S_n}\right)_{se} + \rho_s \left[1 - \left(\frac{S_o}{S_n}\right)_{se}\right] \quad\text{.........................................(2.13)}$$

## 2.5 Well Location

There are two cases to be considered when studying the location of new wells and the use of existing wells as injectors or producers, depending on whether recycling starts after a long period of natural depletion or is planned from the discovery of the field. In the first case the field is already developed, thus the physical characteristics and the geometry of the field are reasonably well known.

In the second case an additional parameter is available for use in the model study; the coordinates of the wells to be drilled. On the other hand, the reservoir limits are ill-defined and the well capacities unknown. As a first step, a model is constructed using the available geological maps, generally assuming that the reservoir has lateral

12

homogeneity. The well capacities are taken to be proportional to the reservoir thickness, unit capacity being based on the results of production tests on the discovery well. The optimum arrangement of wells is then selected, being that which will give the highest recovery for the lowest investment [6].

The relative location of injection and production wells depends on the geology of the reservoir, its type, and the volume of hydrocarbon-bearing rock required to be swept in a time limited by economics. A wide variety of injection-production well arrangements are shown in Figure 2.3.

Some of them, such as the two-spot and three-spot, are isolated well arrangements for possible pilot flooding purposes. The rest are largely portions of repeating injection-producing well patterns. Note that the regular four-spot and inverted-seven spot patterns are identical. The patterns termed inverted have only one injection well per pattern. This is the difference between normal and inverted well arrangements [7].
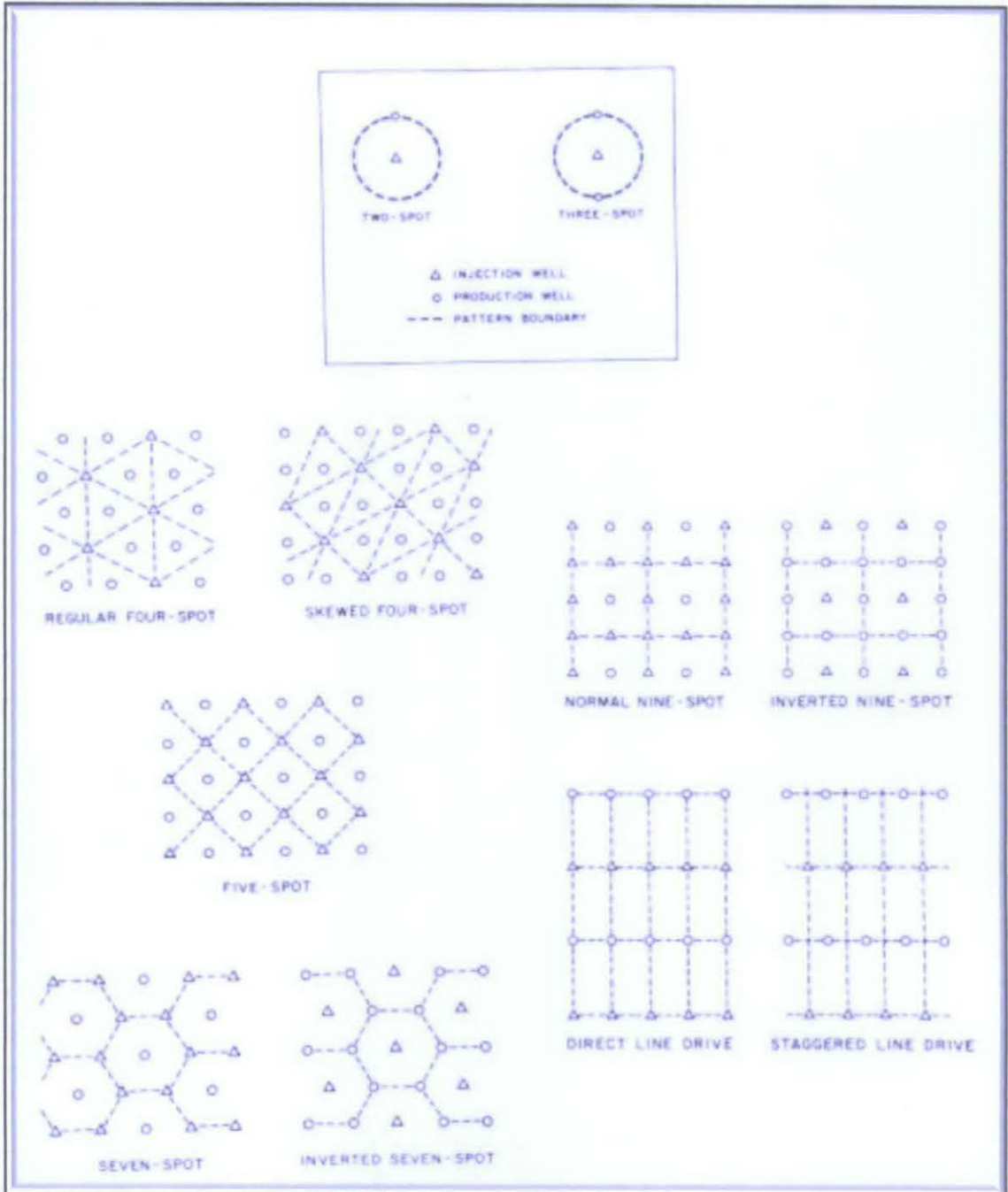
Figure 2.3: Flooding patterns (Craig Jr, 2004)

## 2.6 Well Spacing

Well spacing is defined as an estimated area being drained by a production well [4]. Well spacing can be further categorized into two which are spacing between like wells, *a* and also spacing between adjacent wells, *d* (as shown in Figure 2.4). The spacing for both five spot and seven spot was decided under reservoir condition and can be determined by simple mathematical correlation.
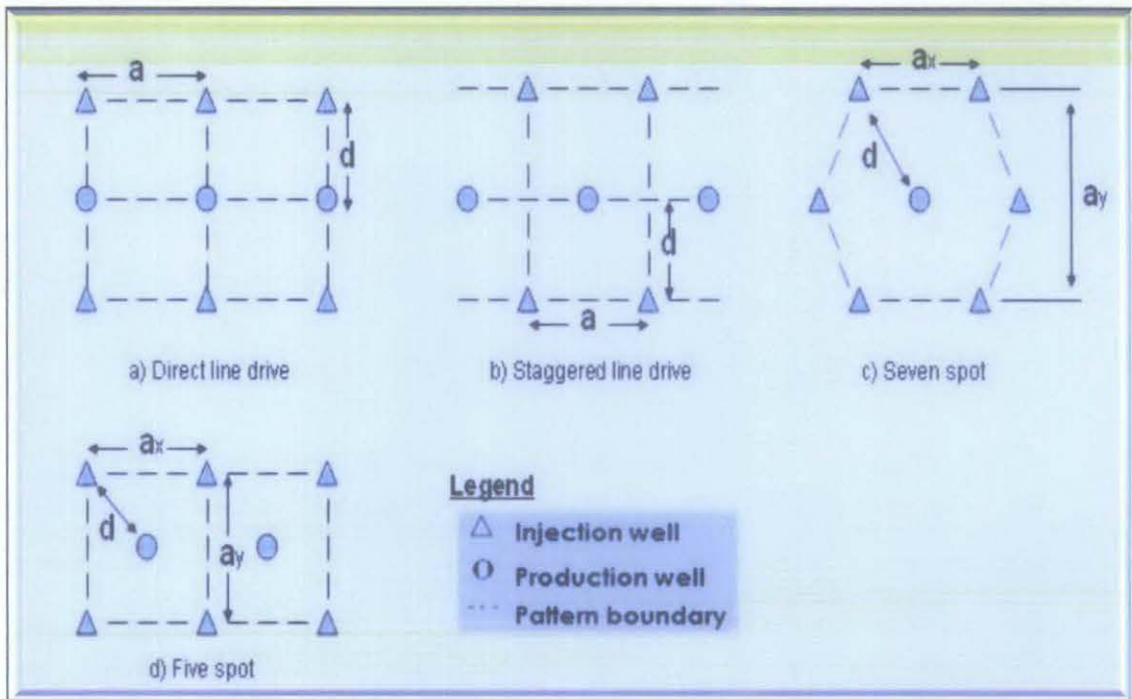


Figure 2.4: Well spacing estimation (i) five spot pattern (ii) seven spot pattern

Based on Figure 2.4 above, the value of *d* for both the five and the seven spot patterns can be obtained using theorem as follow:

$$d = \sqrt{\left(\frac{a_x}{2}\right)^2 + \left(\frac{a_y}{2}\right)^2} \quad \dots \dots \dots \dots \dots \dots \dots \dots \dots \dots \dots \dots \dots \dots \dots \dots \dots \dots (2.14)$$

Meanwhile for the direct and staggered line drive, the value of $a$ and $d$ are equal and was determined based on the geometry of the reservoir, being that the optimum spacing would yield the highest recovery.

A reduction in well spacing requires an increase in the density of production wells. The density of production wells is the number of production wells in a specified area. Well density can be increased by drilling additional wells in the space between wells in a process called infill drilling. Infill drilling is an effective means of altering flow patterns and improving recovery efficiency, but can be more expensive than a fluid displacement process [1].

Apart from the well spacing, the patterns area can also be determined as shown in the following Figure 2.5. Similarly, the patterns area is determined from mathematical correlation as shown in the appendix.
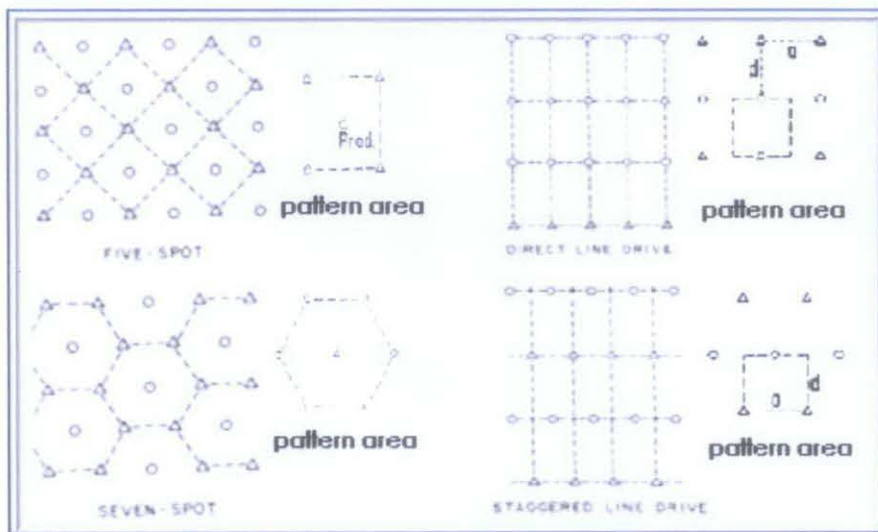


Figure 2.5: Pattern areas of (a) five spot, (b) seven spot, (c) direct line drive and (d) staggered line drive

## 2.7 Mobility Ratio

In Darcy's law there is a proportionality factor relating the velocity of a fluid to the pressure gradient. This proportionality factor, termed the mobility of the fluid, is the effective permeability of the rock to that fluid, divided by the fluid viscosity. Thus the water mobility is $k_w/\mu_w$ and the oil mobility is $k_o/\mu_o$. The value of mobility is dependent upon the fluid saturation [7].

Muskat [8] first discussed the term that has become known as mobility ratio. Later it was used to relate the water mobility in the water-contacted portion of a waterflood to the oil mobility in the oil bank. Later he presented the steady-state pressure distributions for a number of injection-production well arrangements that is under conditions of a unit mobility ratio [9].

Aronofsky [10], was the first to stress the importance of the effect of mobility ratio on the flood patterns during water encroachment focusing on the effect of mobility ratio on the areal coverage of the water-contacted region at the breakthrough of water to the producing wells. Mobility ratio is defined as the ratio of the oil to the displacing fluid mobility.

$$M = \frac{k_{rw}}{\mu_w} \bullet \frac{\mu_o}{k_{ro}} \quad \text{...............................................................................(2.15)}$$

## 2.8 Sweep Efficiency

Sweep efficiency is important to be determined in order to predict the performance of a reservoir. The term sweep efficiency can be divided further into three which are:

  i.   Areal sweep efficiency
  ii.  Displacement efficiency
  iii. Vertical sweep efficiency

### 2.8.1 Areal Sweep Efficiency

In miscible flooding, gas is injected into some wells and produced from other wells. In an areal sense, injection and production take place at points. As a result, pressure distributions and corresponding streamlines are developed between injection and production wells. In symmetrical well patterns, a straight line connecting the injector and producer is the shortest streamline between these two wells, and as a result, the pressure gradient along this line is the highest. Hence injected gas moving areally along this shortest streamline reaches the producing well before the gas moving along any other streamline. Therefore at the time of breakthrough, only a portion of the reservoir area lying between these two wells is contacted by gas. This contacted fraction is the pattern **areal sweep efficiency, E$_A$** [4].

The areal sweep efficiency is defined as the fraction of the total flood pattern that is contacted by the displacing fluid. It increases steadily with injection from zero at the start of the flood until breakthrough occurs, after which E$_A$ continues to increase at a slower rate. The major factors determining areal sweep are:

i. Fluid mobilities
ii. Pattern type
iii. Areal heterogeneity
iv. Total volume of fluid injected

### 2.8.2 Displacement Efficiency

The **displacement efficiency E$_D$** is the fraction of movable oil that has been displaced from the swept zone at any given time or pore volume injected [4]. Mathematically, the displacement efficiency can be expressed conveniently in terms of solvent saturation.

$$E_D = \frac{\overline{S}_s - S_{si} - S_{gi}}{1 - S_{si} - S_{gi}} \quad\text{.................................................................(2-16)}$$

18

where

$S_i$ = average solvent saturation in the swept area

$S_{gi}$ = initial gas saturation at the start of the flood

$S_{si}$ = initial solvent saturation at the start of the flood

Assuming there is no initial gas present at the start of the flood, equation above is reduced to:

$$E_D = \frac{\overline{S}_i - S_{si}}{1 - S_{si}} \dots\dots\dots\dots\dots\dots\dots\dots\dots\dots\dots\dots\dots\dots\dots\dots\dots\dots\dots(2.17)$$

Hence, in order to find the average solvent saturation of the Angsi I-35 reservoir, Buckley-Leverett and Koval method is adopted. Koval method is a mathematical treatment of viscous fingering analogical to the Buckley-Leverett calculation method for immiscible displacement under the condition of the growth of multiple viscous fingers that is not affected appreciably by transverse dispersion [11]. The Buckley-Leverett expression for fractional flow in an immiscible water/oil displacement with negligible gravity and capillary pressure influence is:

$$f_w = \frac{1}{1 + \dfrac{k_o}{k_w} \bullet \dfrac{\mu_w}{\mu_o}} \dots\dots\dots\dots\dots\dots\dots\dots\dots\dots\dots\dots\dots\dots\dots\dots\dots\dots\dots(2.18)$$

where $k_o$ and $k_w$ are permeabilities to oil and water. Koval assume that fractional flow could be expressed by a similar equation for segregated miscible displacement. He reasoned that permeability to either solvent or oil could be expressed as the total permeability multiplied by the average saturation of each fluid and that solvent fractional flow could be calculated as follows when viscous fingering predominates.

$$f_s = \frac{1}{1 + \dfrac{(1 - S_{s)}}{S_s} \bullet \left(\dfrac{\mu_{s_{eff}}}{\mu_{o_{eff}}}\right)\left(\dfrac{1}{H}\right)}$$

19

$$f_s = \cfrac{1}{1 + \cfrac{(1-S_s)}{S_s} \bullet \cfrac{1}{EH}} \quad \dots\dots\dots\dots\dots\dots\dots\dots\dots\dots\dots\dots\dots\dots\dots\dots(2.19)$$

where

$\mu_{s_{eff}}, \mu_{o_{eff}}$ = the effective viscosities in the solvent and oil fingers, cp

E = effective viscosity ratio between the forward-projecting solvent fingers and backward-projecting oil fingers

H = a heterogeneity factor characterizing the heterogeneity of a given rock sample

### 2.8.3 Vertical Sweep Efficiency

The **vertical sweep efficiency** $E_V$ is the fraction of the vertical section of the pay zone that is contacted by injected fluids. This particular sweep efficiency depends primarily on the mobility ratio and total volume injected. As a consequence of the nonuniform permeabilities, any injected fluid will tend to move through the reservoir with an irregular front. The area of the greatest uncertainty in designing a flooding is the quantitative knowledge of the permeability variation within the reservoir. The degree of permeability variation is considered by far the most significant parameter influencing the vertical sweep efficiency. Stiles [12] proposed that the vertical sweep efficiency can be calculated from the following expression assuming that the reservoir is composed of an idealized layered system.

$$E_V = \cfrac{k_i \sum_{j=1}^{i} h_j + \sum_{j=i+1}^{n} (kh)_j}{k_i h_t} \quad \dots\dots\dots\dots\dots\dots\dots\dots\dots\dots\dots\dots\dots\dots\dots\dots(2.20)$$

where

i = breakthrough layer

n = total number of layers

$E_V$ = vertical sweep efficiency

$h_t$ = total thickness, ft

$h_i$ = layer thickness, ft

## 2.9 Recovery Factor

The effect of well patterns with different spacing to water alternating carbon dioxide gas injection can be estimated in term of overall recovery factor, RF. The overall recovery factor of any secondary or tertiary oil recovery method is the product of a combination of three individual efficiency factors as given by the following generalized expression:

$$R_f = E_A \times E_d \times E_v \quad\text{.................................................................}(2.21)$$

where

        $E_A$ = areal sweep efficiency

        $E_V$ = vertical sweep efficiency

        $E_d$ = displacement efficiency

# CHAPTER 3

# METHODOLOGY

## 3.1 Project Flow Chart

The following figure shown is the project flow chart showing the works done in order to complete the project:
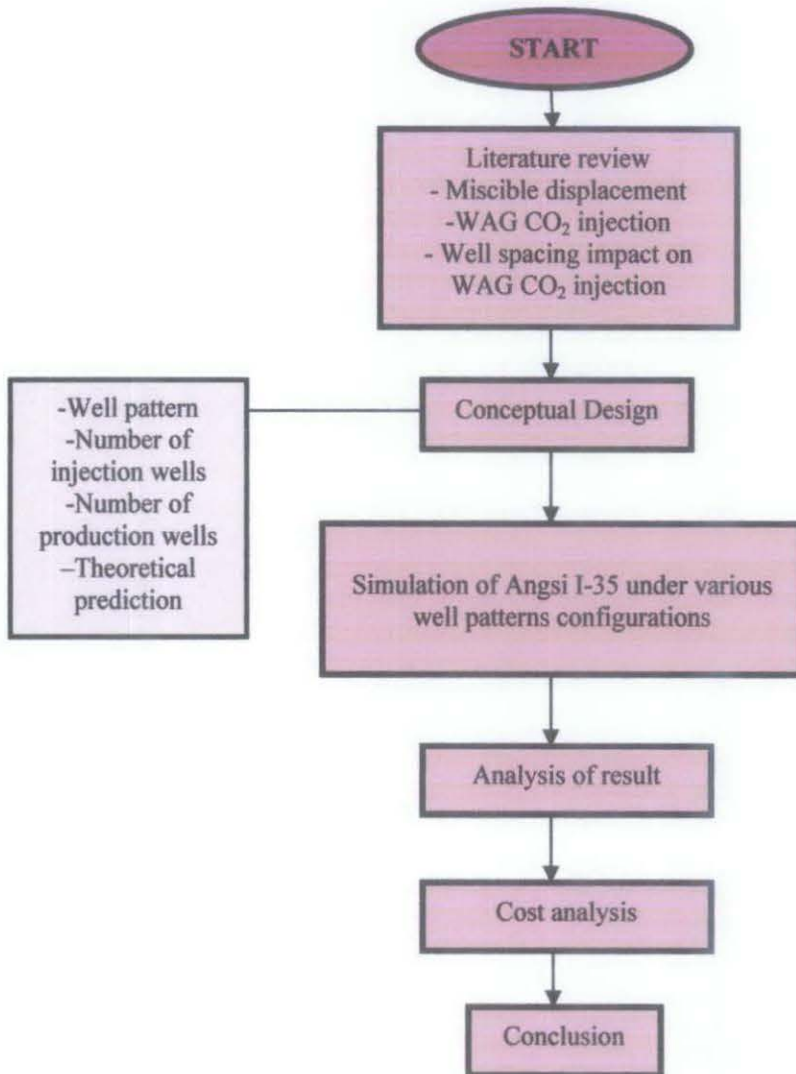


Figure 3.1: Project flow chart

## 3.2 Project Activities and Key Milestone

### 3.2.1 Literature Review

The project started with literature review on miscible displacement process. It was then commenced to carbon dioxide water alternating gas (WAG) injection with the purpose of studying and understanding the effect of well patterns with different spacing to WAG $CO_2$ injection. The main sources for the review were mostly from SPE journal and related books.

### 3.2.2 Conceptual Design

The conceptual design phase focused on determining the spacing of the wells in the specified patterns selected. The selected well patterns were (as shown in figure 2.3):

  i.    five spot – **(case A)**
  ii.   seven spot – **(case B)**
  iii.  inverted seven spot – **(case C)**
  iv.   direct line drive – **(case D)**
  v.    staggered line drive – **(case E)**

The task included on deciding the number of injection and production wells to be employed in the patterns, which was supported by theoretical prediction and calculation. The theoretical works involve are:

  i.    Determine the spacing of wells for each cases
  ii.   Calculating the mobility ratio of the reservoir at reservoir pressure
  iii.  Approximation of areal sweep efficiency from graph as shown in appendix at mobility ratio
  iv.   Calculating the displacement efficiency from $CO_2$ saturation
  v.    Estimating the vertical sweep efficiency

vi.   Computing the recovery factor which is the product of the three efficiencies for each cases

Upon doing the theoretical prediction, several assumptions were made which were:

i.    the reservoir was a homogenous porous media

ii.   there was no initial gas present at the start of the flood

### 3.2.3   Simulation of Angsi I-35

Simulation was performed using a black oil simulator. Figure 3.2 illustrated the original Angsi I-35 reservoir simulated on FloViz.
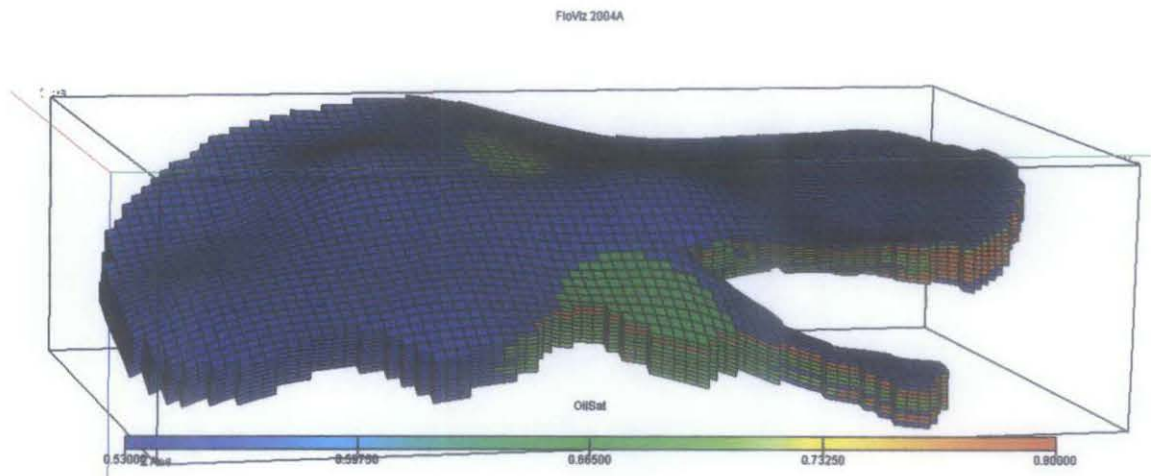


Figure 3.2: Angsi I-35 reservoir

Figure 3.3 demonstrated the allocated wells on Angsi I-35 for case A utilizing the five spot well pattern. The allocation of injection wells and production wells and also the spacing between them were restricted to the reservoir geometry.
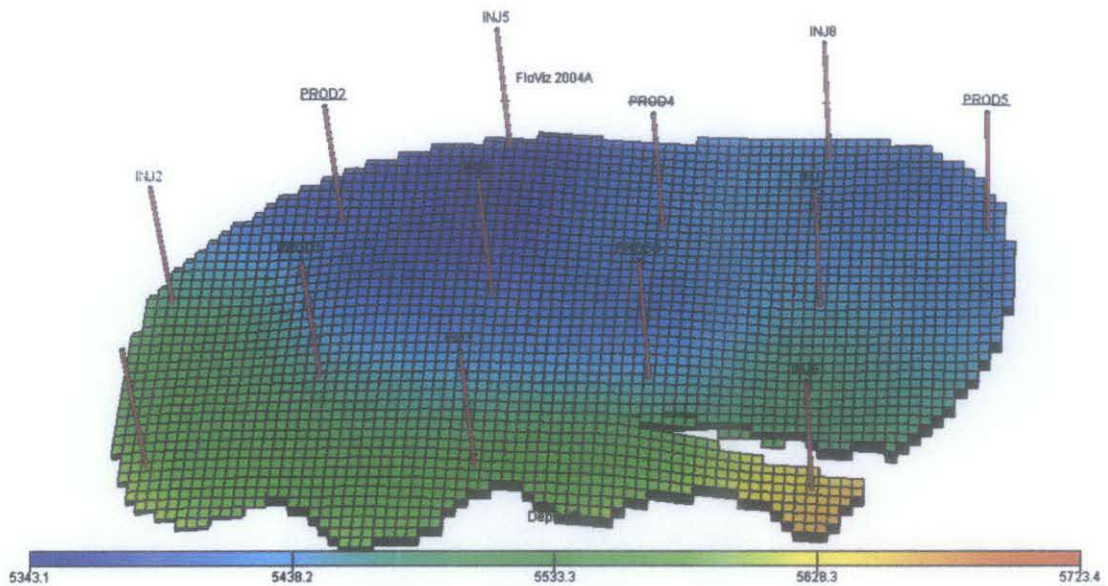
24

Figure 3.3: Example of wells allocation for Angsi I-35 simulation

Several assumptions were made during the simulation which were:

i.   the forecasted production years was for 30 years

ii.  alternating six months period of water injection and $CO_2$ injection was implemented between them for the whole 30 years

### 3.2.4   Analysis of Result

The simulation results were already obtained and it was then being compared to the theoretical result to see whether both results were similar or different. The overview of the best well patterns for Angsi I-35 could be predicted but yet it still had to be justified in term of cost to get the most optimum one.

### 3.2.5   Cost Analysis

The final phase of the project was computing cost analysis for all the five well patterns. The objective for executing cost analysis was to investigate each well pattern and find the one that required the lowest expenditure. This expenditure was evaluated in terms of unit technical cost for each cases of well patterns studied.

Upon computing the cost analysis, several assumptions had to be made which were:

  i.    CAPEX cost quantified for each well patterns is only for the total cost of production wells and injection wells

  ii.   5% inflation and 30% contingencies are included in the CAPEX calculation

  iii.  the cost for production well is USD4.86 million/unit and the cost for each injection well is USD6.69 million/unit

# CHAPTER 4

# RESULT AND DISCUSSION

## 4.1 Theoretical Prediction

The followings are the theoretical work done upon completing the project, which later to be compared with the simulation result from Eclipse 100. The best well patterns for Angsi I-35 reservoir is determined in termed of the value of recovery factor with respect to number of injection and production wells which will be included as the project progress further in cost estimation.

### 4.1.1 Well Spacing

For case A, case B and case C their well spacing can be obtained using the mathematical correlation shown below (equation 2.14):

$$d = \sqrt{\left(\frac{a_x}{2}\right)^2 + \left(\frac{a_y}{2}\right)^2}$$

i.   For case A:

$$d = \sqrt{\left(\frac{5904}{2}\right)^2 + \left(\frac{9840}{2}\right)^2}$$

$$d = 5737.66 \, ft$$

ii.   For case B and case C:

$$d = \sqrt{\left(\frac{7872}{2}\right)^2 + \left(\frac{7872}{2}\right)^2}$$

$$d = 5566.34 \, ft$$

For both case D and case E, their spacing is determined based on the geometry of the reservoir. The adjacent wells for the patterns are located at 5904ft spacing.

Table 4.1: Adjacent well spacing for all well patterns

| Cases | Well spacing, d (ft) |
|---|---|
| Case A | 5737.66 |
| Case B | 5566.34 |
| Case C | 5566.34 |
| Case D | 5904.00 |
| Case E | 5904.00 |

### 4.1.2 Mobility Ratio

At pressure of P = 3420psia (reservoir pressure), properties of Angsi I-35 are:

Table 4.2: Properties of Angsi I-35 at pressure P=3420psia

| Property | Value |
|---|---|
| Water viscosity, $\mu_w$ | 0.32cp |
| Oil viscosity, $\mu_o$ (value obtained from Figure 4.1) | 1.55cp |
| Oil relative permeability, $k_{ro}$ (value obtained from Figure 4.2) | 0.92 |
| Water relative permeability, $k_{rw}$ (value obtained from Figure 4.2) | 0.40 |

The data of oil viscosity versus pressure for Angsi I-35 is shown in Figure 4.1. From this figure, the value of oil viscosity at prevailing reservoir pressure of 3420psi can be found.
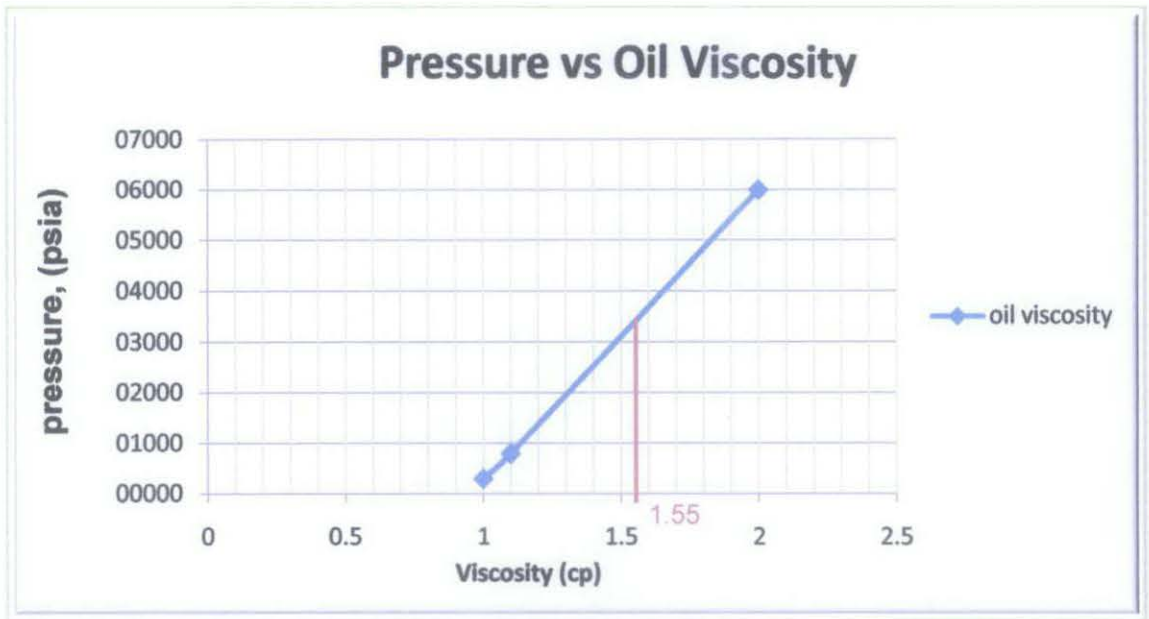
Figure 4.1: Viscosity of oil at pressure, P = 3420psia

The relative permeability data of Angsi I-35 is shown in a graph on Figure 4.2.
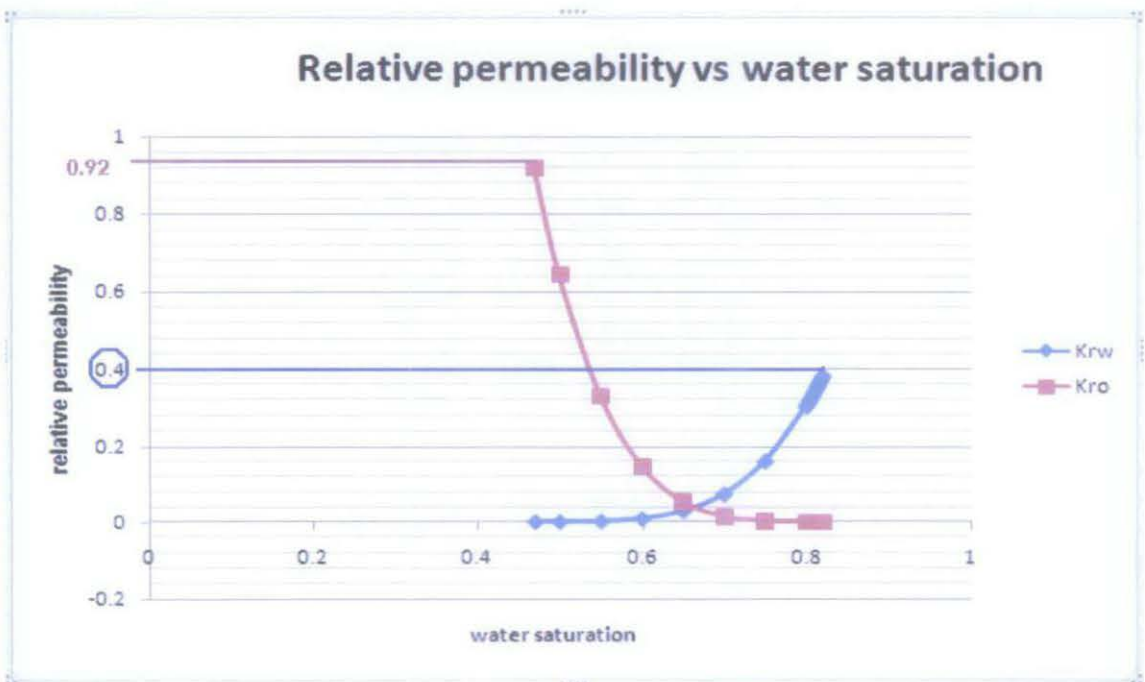


Figure 4.2: Relative permeability of water and oil with respect to water saturation

Hence, mobility ratio is (equation 2.15):

$$M = \frac{k_{rw}}{\mu_w} \bullet \frac{\mu_o}{k_{ro}}$$

$$M = \frac{0.40}{0.32} \times \frac{1.55}{0.92}$$

$$\underline{M = 2.1}$$

### 4.1.3 Areal Sweep Efficiency

The values of areal sweep efficiency, $E_A$ can be determined from figures shown in appendix which are being determined at mobility ratio of 2.1. The values of areal sweep efficiency for each pattern are listed in descending order in Table 4.3.

Table 4.3: Percentage of areal sweep efficiency at mobility ratio = 2.1

| Cases | Areal sweep efficiency (%) |
|---|---|
| Case B | 68 |
| Case C | 66 |
| Case E | 65 |
| Case A | 60 |
| Case D | 50 |

### 4.1.4 Displacement Efficiency

The effective viscosity ratio is different from the nominal viscosity ratio of pure oil and solvent because of solvent/oil mixing in the fingered region. Assuming homogeneous porous media the effective viscosity ratio is:

$$E = \left[ 0.78 + 0.22 \left( \frac{\mu_o}{\mu_s} \right)^{\frac{1}{4}} \right]^4 \quad \text{.............................................(4.1)}$$

where $\mu_o$ and $\mu_s$ are the viscosities of pure oil and solvent.

30

$$E = \left[ 0.78 + 0.22 \left( \frac{1.55}{0.045} \right)^{\frac{1}{4}} \right]^4$$

$$E = 2.97$$

The viscosity of solvent ($CO_2$) used in equation 4.1 above can be found as shown in the graph in Figure 4.3.
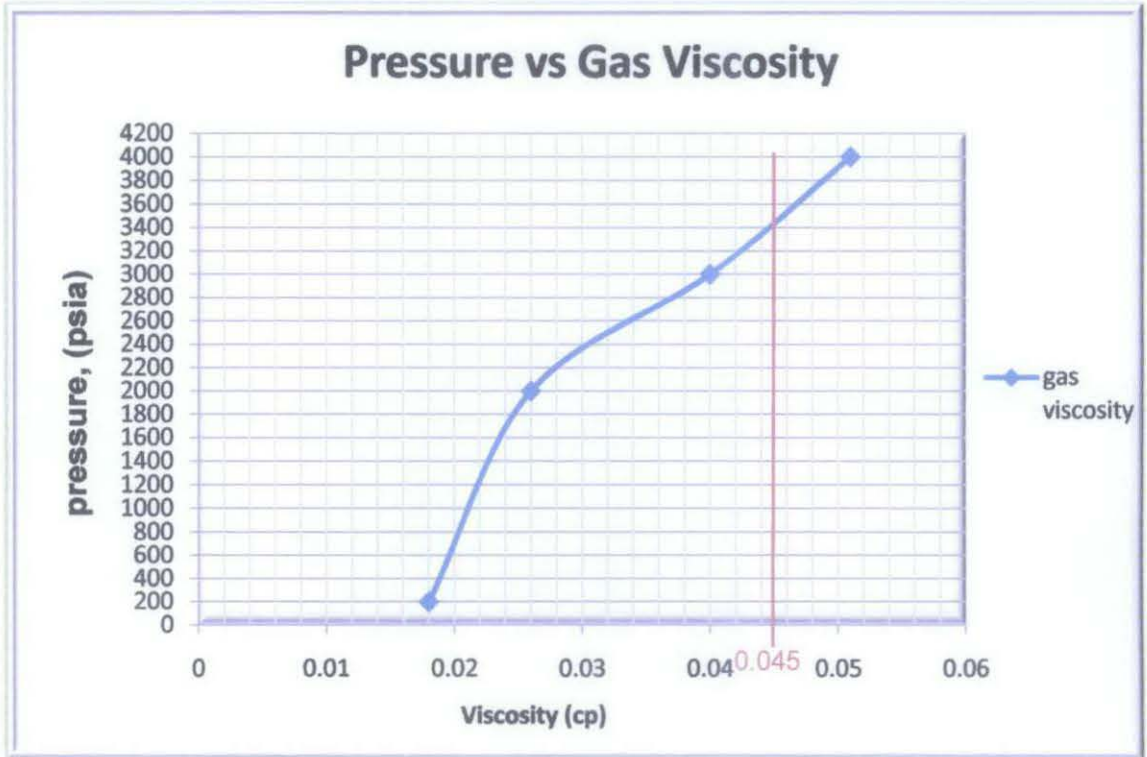


Figure 4.3: Viscosity of carbon dioxide ($CO_2$) at pressure, P = 3420psia

Hence, the solvent fractional flow can be calculated using Equation 2.19 by assuming the fluid is homogenous, H = 1.

$$f_s = \cfrac{1}{1 + \cfrac{(1-S_s)}{S_s} \bullet \cfrac{1}{(2.97)(1)}} \dots\dots\dots\dots\dots\dots\dots\dots\dots\dots\dots\dots\dots(4.2)$$

31

Substituting the value of $CO_2$ saturation from appendix into equation 4.2 to get the value of fractional flow and computing the fractional flow curve graph, the value of average solvent saturation can be obtained as shown in Figure 4.4.

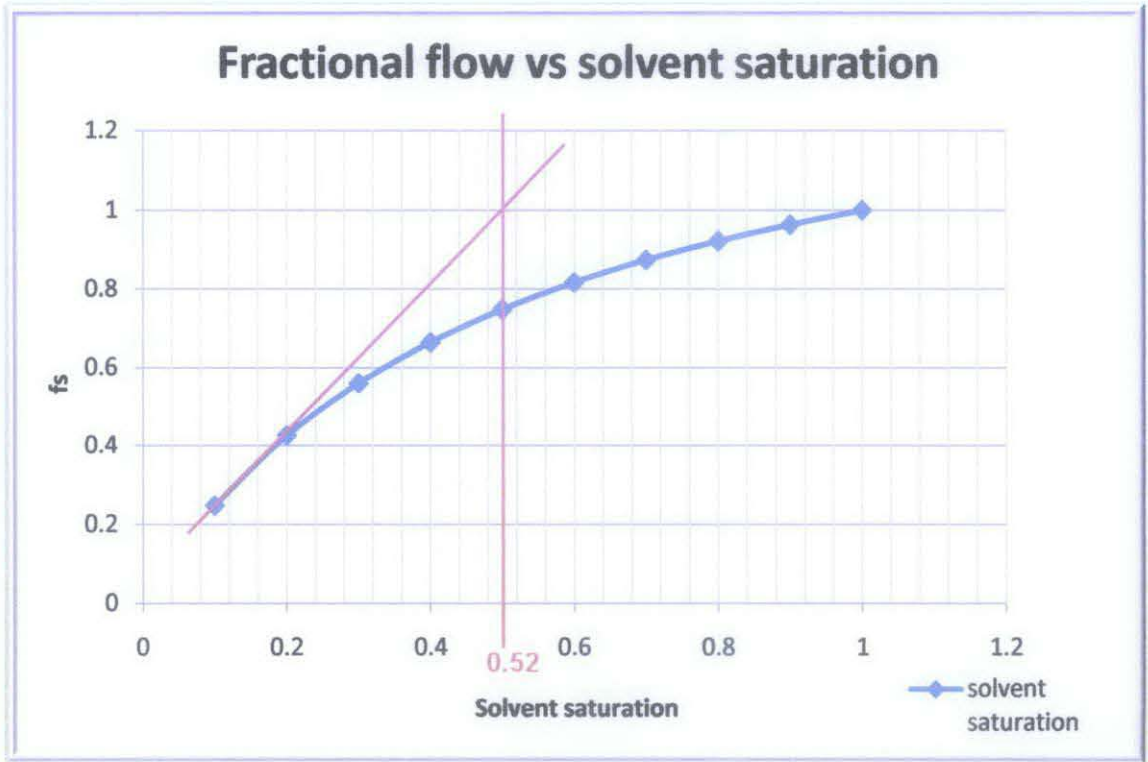**Fractional flow vs solvent saturation**

Figure 4.4: Fractional flow curve

The value of average solvent saturation is then substituted into equation 2.17 to get the value of displacement efficiency.

$$E_D = \frac{\overline{S}_i - S_{si}}{1 - S_{si}}$$

$$E_D = \frac{0.52 - 0.1}{1 - 0.52}$$

$$E_D = 0.875$$

$$\underline{E_D = 87.5\%}$$

### 4.1.5 Vertical Sweep Efficiency

The value of vertical sweep efficiency is equivalent to 100% since assumption is made that the reservoir is homogenous for the theoretical calculation stage.

### 4.1.6 Overall Recovery Factor

From the results calculated earlier, the recovery factor for each of the cases can be determined from equation 2.21. The values obtained are shown in Table 4.4.

Table 4.4: Percentage of recovery factor for all five cases

| Cases | Recovery factor (%) |
|-------|---------------------|
| Case B | 59.50 |
| Case C | 57.75 |
| Case E | 56.88 |
| Case A | 52.50 |
| Case D | 43.75 |

### 4.1.7 Summary of Results

Table 4.5 illustrates the summary of results for the theoretical works done on predicting the effect of well patterns to the Angsi I-35 reservoir.

Table 4.5: Results summary of theoretical works done on Angsi I-35

| Cases | Spacing between like wells, a (ft) | Spacing between adjacent wells, d (ft) | Pattern area (ft²) | Areal sweep efficiency, $E_A$ (%) | Displacement efficiency, $E_d$ (%) | Vertical sweep efficiency, $E_V$ (%) | Recovery factor (%) |
|-------|------|------|------|------|------|------|------|
| Case B | 7872 x 7872 | 5566.34 | 92952576 | 68 | 87.5 | 100 | 59.50 |
| Case C | 7872 x 7872 | 5566.34 | 92952576 | 66 | 87.5 | 100 | 57.75 |
| Case E | 5904 x 5904 | 5904.00 | 34857216 | 65 | 87.5 | 100 | 56.88 |
| Case A | 5904 x 9840 | 5737.66 | 58095360 | 60 | 87.5 | 100 | 52.50 |
| Case D | 5904 x 5904 | 5904.00 | 34857216 | 50 | 87.5 | 100 | 43.75 |

The theoretical results show that case B (seven spot) well pattern offers the best option as it yield the highest recovery among all cases. This indicates that spacing of 5566.34ft between adjacent wells is the best well spacing for Angsi I-35 with 59.50% of oil recovery. Meanwhile, case D which represents direct line drive well pattern offers the lowest oil recovery among all cases at 43.75% with adjacent well spacing of 5904ft. The results summarized in Table 4.5 above were arranged in descending order of recovery factor with their respective well spacing stated.

## 4.2 Simulation Result

For the project, simulation was conducted in order to justify the theoretical result obtained earlier. Table 4.6 depicts the quantity of injection wells and production wells employ for each cases.

Table 4.6: Number of wells employ on each cases of well pattern

| Cases | Number of injection well | Number of production well |
|---|---|---|
| Case A | 8 | 5 |
| Case B | 9 | 3 |
| Case C | 3 | 9 |
| Case D | 5 | 5 |
| Case E | 5 | 4 |

Additionally, the followings are the result obtained after the simulation finished.

### 4.2.1 Oil Recovery

Oil recovery efficiency can be measured in term of field oil efficiency (FOE) which is a fraction of produced oil to the initial oil in the reservoir. FOE is defined as:

$$FOE = \left[ \frac{(OIP_{initial} - OIP_{now})}{OIP_{initial}} \right] \dots\dots\dots\dots\dots\dots\dots\dots\dots\dots\dots\dots\dots\dots\dots(4.3)$$

where OIP indicates oil in place. Figure 4.5 below shows the result obtained after the simulation for each well pattern. The value of FOE for each case was obtained at HCPV value of 1.
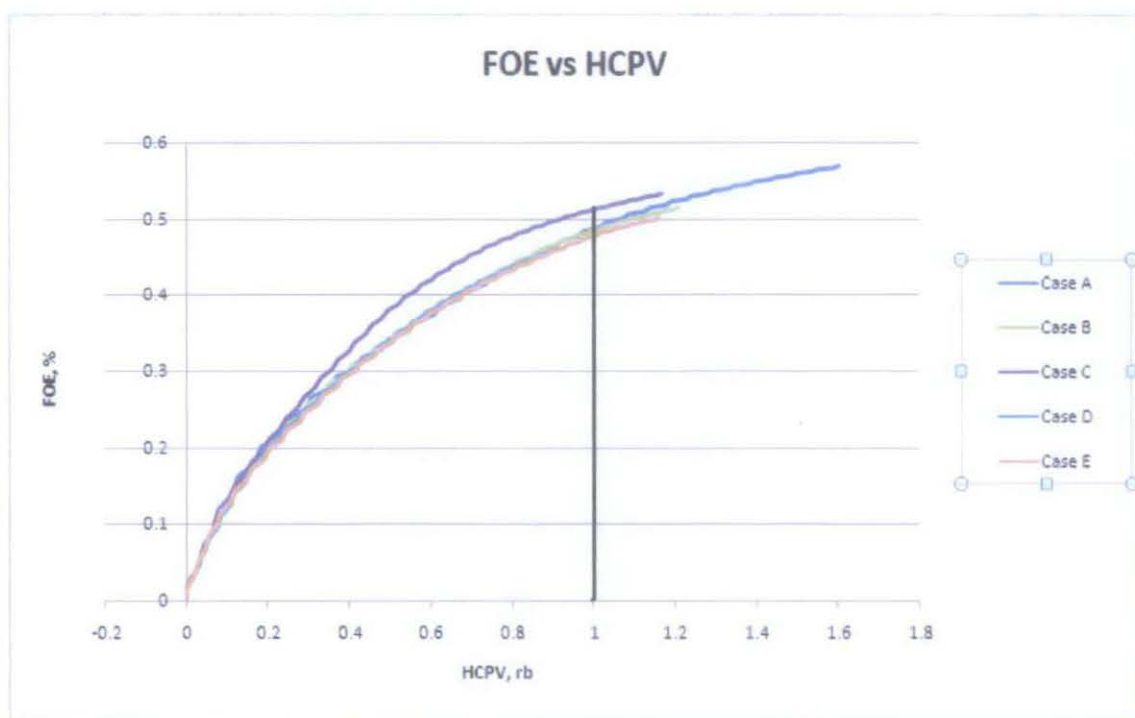
Figure 4.5: Graph of FOE versus HCPV at the end of 1 pore volume injection

Table 4.7: Value of FOE for all five well patterns

| Cases | FOE (%) |
|-------|---------|
| Case C | 52.0 |
| Case A | 48.0 |
| Case B | 47.5 |
| Case E | 46.0 |
| Case D | 45.5 |

Table 4.7 represents the oil recovery result for all cases from the highest recovery to the lowest in descending sequence. Case C (inverted seven spot) well patterns with adjacent well spacing of 5566.34ft yield the highest FOE of 52%. This is followed by case A (five spot), case B (seven spot), case E (staggered line drive) and lastly case D (direct line drive) well pattern with 45.5% oil recovery. The difference between the highest value of FOE and the lowest is in the range of 6.5%.
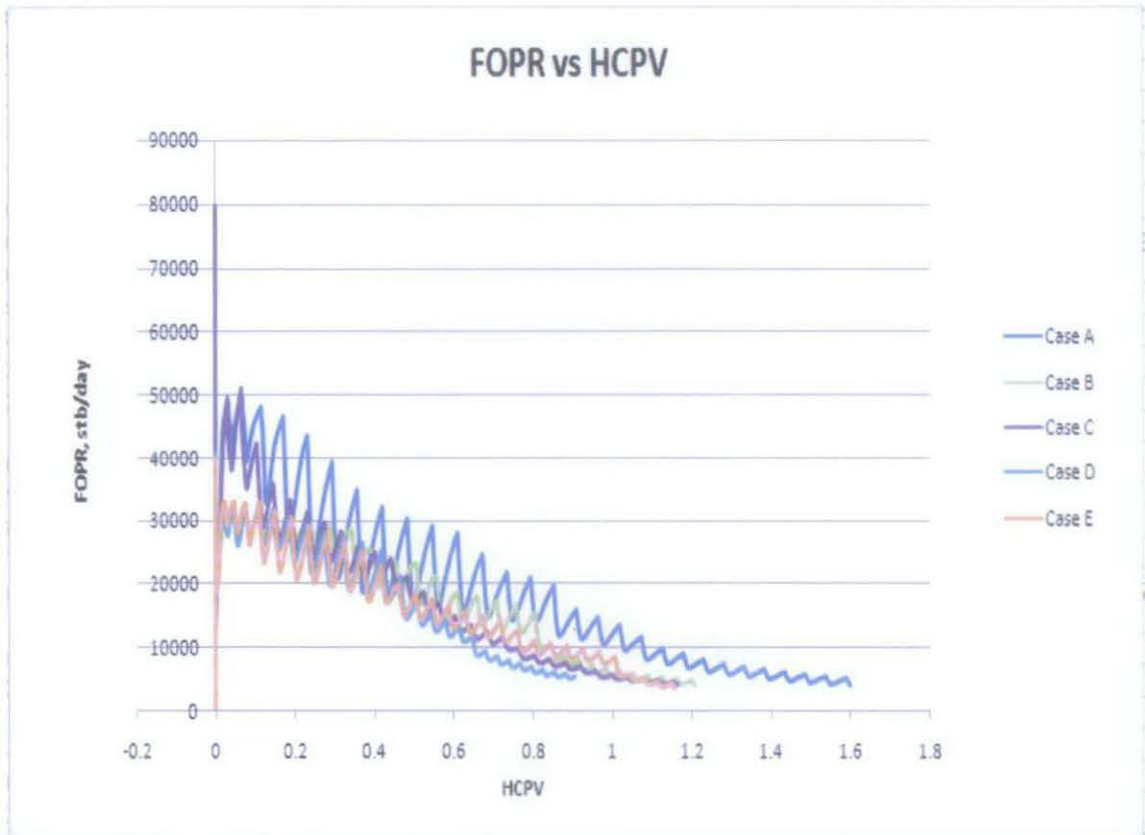
## 4.2.2 Production Rate



Figure 4.6: Graph of FOPR versus HCPV

As shown in Figure 4.6, generally the production rate for all five patterns is alternating. The figure illustrates that case A (five spot) demonstrates the highest production rate towards the end among the five configurations. However, during the early days of the recovery the production rate for inverted seven spot well pattern is the highest among all.

## 4.3 Comparison between theoretical and simulation result



**Comparison of oil recovery between theoretical and simulation**

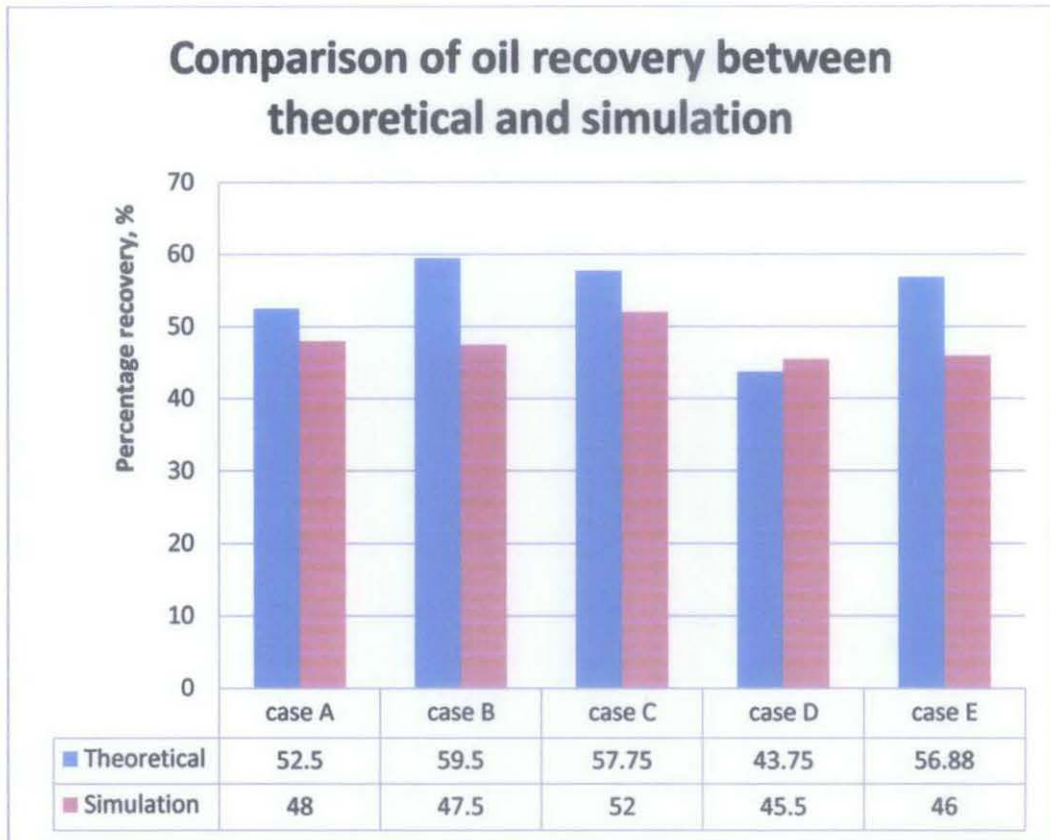| | case A | case B | case C | case D | case E |
|---|---|---|---|---|---|
| ■ Theoretical | 52.5 | 59.5 | 57.75 | 43.75 | 56.88 |
| ■ Simulation | 48 | 47.5 | 52 | 45.5 | 46 |

Figure 4.7: Comparison of oil recovery between theoretical result and simulation result

The above figure shows that there are differences between the theoretical result and the simulation result obtained. For the theoretical result, it shows that case B (seven spot) yield the highest recovery whereas for the simulation result the highest oil recovery is from case C which represents inverted seven spot well pattern. Meanwhile for the lowest oil recovery, it indicates the same result from both methods though the value is slightly different.

The differences between the results are due to assumption made upon conducting each method. For the theoretical method, assumption was made that the Angsi I-35 reservoir is homogenous whereas in real, Angsi I-35 comprises 11 layers with different permeability for each layers. Hence, the value of vertical sweep efficiency cannot be

equal to 100%. Furthermore, the calculation for the theoretical works is based on water flooding and miscible flooding model. Thus, it is more suitable to both flooding model compare to WAG $CO_2$ injection implemented to complete the simulation and consequently the objective of the project.

## 4.4 Cost Estimation

Cost estimation was done in order to find the most optimum well pattern for Angsi I-35 reservoir being that optimum is defined as substantial oil recovery with the lowest expenditure. Hence, the findings of the project are presented in the following sections.

### 4.4.1 Unit Technical Cost

Unit technical cost (UTC) which is defined as cost per barrel of production is useful when production is constraint on a project or when making technical comparison between projects in the same geographical area. In the project, comparison is made between well patterns implemented on the same Angsi I-35 reservoir. The formula to find the unit technical cost for each patterns is given as follow:

$$\text{Unit technical cost (UTC)} = \frac{(CAPEX + OPEX) \ (USD/bbl)}{\text{Production}}$$

In the project, case E which represents the staggered line drive well pattern yields the lowest value of UTC at USD3.542/barrel followed by case C (USD4.099/barrel), case D (USD4.218/barrel), case A (USD4.559/barrel) and the highest value of UTC was obtained from case B which represents the seven spot well pattern (USD4.806/barrel). This indicates that case E is the most attractive well patterns to be implemented on Angsi I-35 since it offers the highest profit as its cost per barrel of production is the lowest among all cases. The results were presented on Figure 4.8 and Table 4.8 in ascending value of UTC.

39

# Unit technical cost vs cases

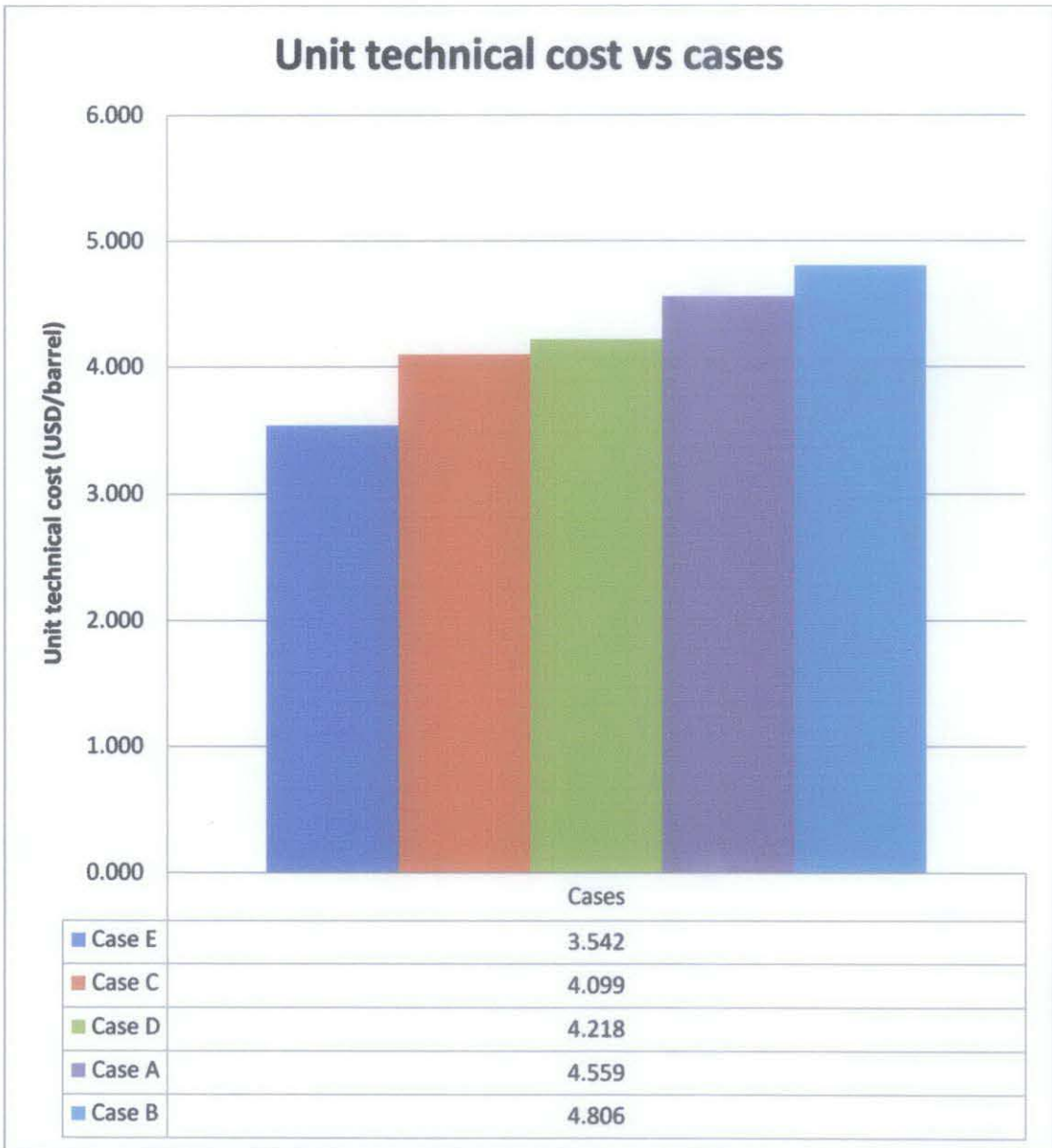| Cases | |
|---|---|
| ■ Case E | 3.542 |
| ■ Case C | 4.099 |
| ■ Case D | 4.218 |
| ■ Case A | 4.559 |
| ■ Case B | 4.806 |

Figure 4.8: Graph of unit technical cost versus each case of well patterns

Table 4.8: Value of UTC for all five well patterns

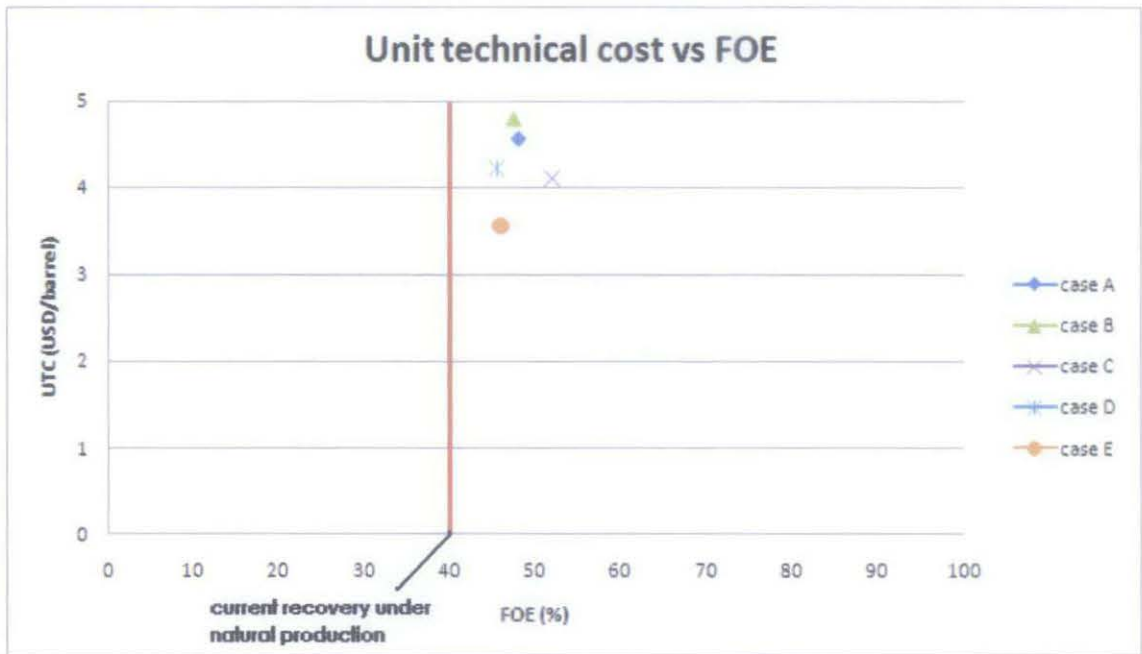| Cases | Unit technical cost (USD/barrel) |
|---|---|
| Case E | 3.542 |
| Case C | 4.099 |
| Case D | 4.218 |
| Case A | 4.559 |
| Case B | 4.806 |

Figure 4.9: Unit technical cost with respect to oil recovery

Figure 4.9 shows the value of UTC with respect to oil recovery for each well pattern. From the figure, it illustrates that all the value of FOE for the five cases lies above the value of current recovery under natural production, which is at 0.4. This justifies that all the five well configurations are practical in terms of offering enhanced oil recovery to Angsi I-35 as the FOE recovered exceed the natural production recovery. In terms of economic, the range of UTC for all five cases lies between USD3.542/barrel to USD4.806/barrel which is about 1.264 differences.

# CHAPTER 5

# CONCLUSION AND RECOMMENDATION

As a conclusion, the objective of the project which is to study the effect of well patterns to the WAG $CO_2$ injection on Angsi I-35 reservoir was achieved. The implementation of the well patterns with each having different well spacing is listed as below:

 i.  Five spot pattern – 8 injection wells and 5 production well

 ii.  Seven spot pattern – 9 injection wells and 3 production wells

 iii.  Inverted seven spot pattern – 3 injection wells and 9 production wells

 iv.  Direct line drive pattern – 5 injection wells and 5 production wells

 v.  Staggered line drive pattern – 5 injection wells and 4 production wells

Those patterns are normally use worldwide for flooding processes which make them feasible to employ on this project.

From the project, conclusion can be made as follows:

 i.  The highest amount of oil recovery was obtained from inverted seven spot well pattern with 52%, which was about 12% more from the current recovery under natural production

 ii.  The most profitable well patterns was staggered line drive well pattern which yield the lowest value of unit technical cost at USD3.542/barrel and the least profitable option was seven spot well pattern as it lays the highest value of UTC at USD4.806/barrel

iii.    All five well patterns are proved to be feasible to implement on Angsi I-35 reservoir as the oil recovery from each patterns exceeds the 40% of current oil recovery under natural production

iv.    The optimum well spacing for Angsi I-35, being that it offers reasonable oil recovery at the lowest production cost per barrel was 5904ft of spacing between like wells, and also 5904ft between adjacent wells

On the other hand, there are several ways to improve on the findings of this project such as:

i.    Considering the different permeability of each layer on Angsi I-35 to attain more accurate value of vertical displacement efficiency, hence getting more accurate value of theoretical oil recovery

ii.    Allocate more production wells compare to injection wells to each well pattern to ensure more oil can be produced

iii.    Allocate the same quantity of production wells and injection wells for each well patterns to obtain more accurate comparison in term of oil recovery and profitability

When the natural reservoir energy is judged to be insufficient, the choice of enhanced recovery method is made according to both technical and economic criteria. If more than one method is technically feasible, an economic analysis is performed for each one, comparing the increased revenue (due to the increase in oil recovery) with the additional expenditure required, and the method yielding the highest profit is chosen.

43

# REFERENCES

1. M.Latil, 1980, "Enhanced Oil Recovery", *Editions Technip*, Institut Francais Du Petrole Publications

2. Legal & Corporate Affairs Division PETRONAS, copyright 2000-2001, < http://www.alam.edu.my/internet/corp/news.nsf/2b372bb45ff1ab3a48256b42002 b19a7/3b3c72dd772bbe4048256b350022ced1?OpenDocument>

3. Perry M.Jarrel, Charles E.Fox, Michael H.Stein, Steven L.Webb, 2002, "Practical Aspects of $CO_2$ Flooding", *Monograph Volume 22 SPE, Henry L.Doherty Series*

4. Tarek Ahmed, Second Edition 2001, *Reservoir Engineering Handbook*, Gulf Professional Publisihing

5. Todd M., Longstaff W., 1972, The Development, Testing and Application of a Numerical Simulator for Predicting Miscible Flood Performance, *SPE 3484*

6. J. Scott Moore, 5 Feb 1981, *Well Location Pattern for Secondary and Tertiary Recovery*, Conoco Inc.

7. Forrest F.Craig Jr., Fourth Edition 1993, "The Reservoir Engineering Aspects of Waterflooding", *Monograph Volume 3 of The Henry L.Doherty Series*

8. Muskat, M, 1937: *The Flow of Homogenous Fluids Through Porous Media*, McGraw-Hill Book Co., New York.

9. Muskat, M., 1949: Physical Principles of Oil Production, McGraw-Hill Book Co., New York

10. Aronofsky, J., 1952: "Mobility Ratio, Its Influence on Flood Patterns During Water Encroachment", *Trans., AIME*

11. Fred I. Stalkup Jr., 3$^{rd}$ Printing 1992, *Miscible Displacement,* SPE Monograph Series

12. Stiles, W.E.: "Use of Permeability Distribution in Water Flood Calculations", *Trans., AIME*

13. Rancher Energy, Enhanced Oil Recovery Using Carbon Dioxide, http://www.rancherenergy.com/technology.asp?techID=2

14. Schlumberger, 2008 <http://www.glossary.oilfield.slb.com/Display.cfm?Term=miscible%20displacement>

15. Herbert L.Stone, 10 May 2004, Method for Improved Vertical Sweep of Oil Reservoirs

16. IOR News Letter No. 6, March 1996, http://www.npd.no/engelsk/news/ior6/ior-6.htm

17. Energy Citations Database (ECD) – Document #6857369, http://www.osti.gov/energycitations/product.biblio.jsp?osti_id=6857369

18. Sharp IOR Newsletter, http://ior.senergyltd.com/issue6/articles/BP/magnus_dsh.htm

19. Method for recovery of hydrocarbons – Patent 4715444, http://www.freepatentsonline.com/4715444.html

## CALCULATION OF WELL PATTERNS AREA

**For case A;**

There are 18 grids between like wells along the x-axis and 30 grids between like wells along the y-axis, and each grid constitute 328ft of spacing. Hence, the pattern area can be calculated as follow:

$$PatternArea = (18 \times 328 \, ft) \times (30 \times 328 \, ft)$$

$$PatternArea = 58095360 \, ft^2$$

**For case B and case C;**

There are 24 grids along both x-axis and y-axis, and each grid constitutes 328ft of spacing. Thus, the pattern area is:

$$PatternArea = (24 \times 328 \, ft) \times (24 \times 328 \, ft)$$

$$PatternArea = 92952576 \, ft^2$$

**For case D and case E;**

There are 18 grids along both x-axis and y-axis, and each grid constitutes 328ft of spacing. Thus, the pattern area is:

$$PatternArea = (18 \times 328 \, ft) \times (18 \times 328 \, ft)$$

$$PatternArea = 34857216 \, ft^2$$

WELLS ALLOCATION FOR CASE B (SEVEN SPOT) PATTERN
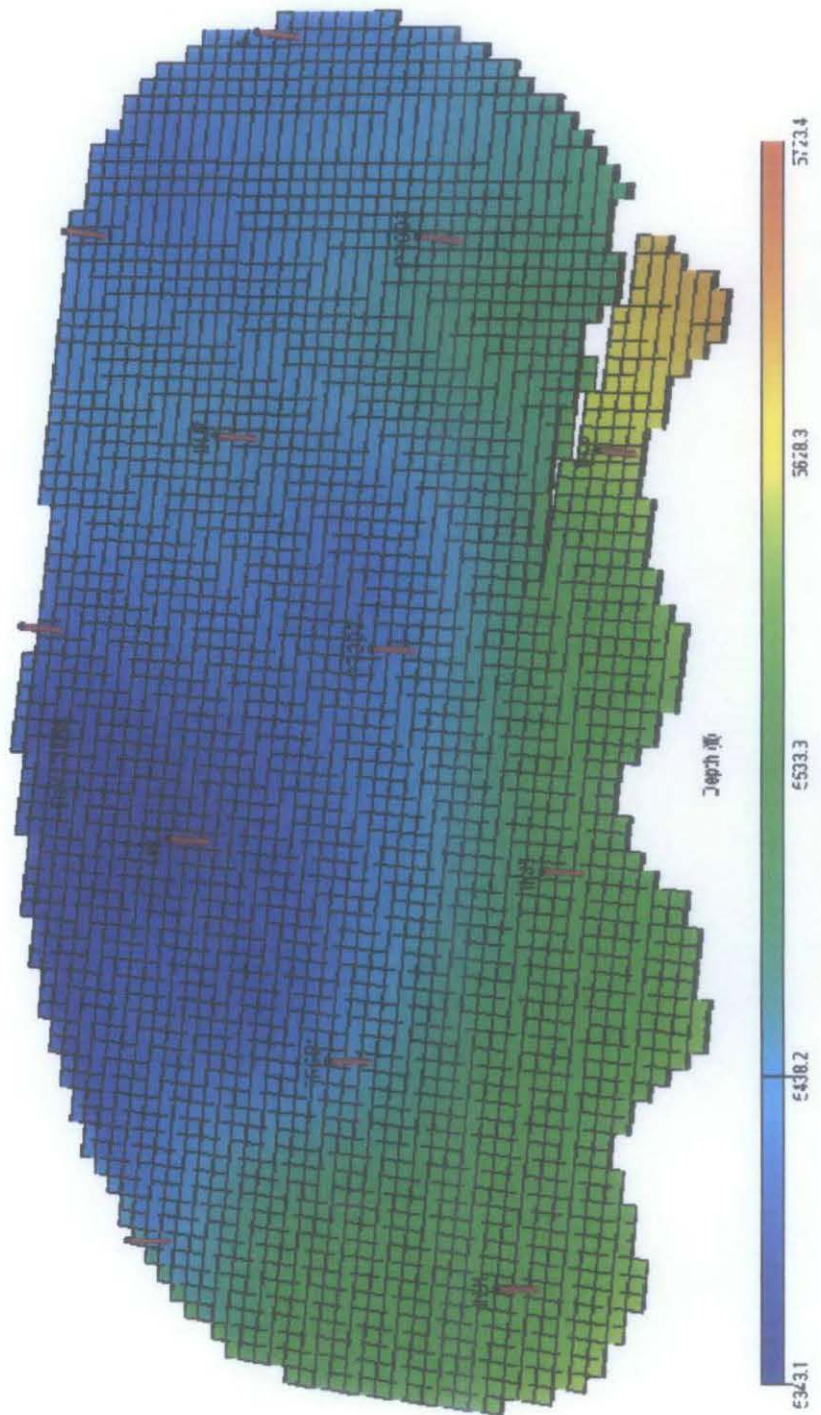
# WELLS ALLOCATION FOR CASE C (INVERTED SEVEN SPOT) PATTERN
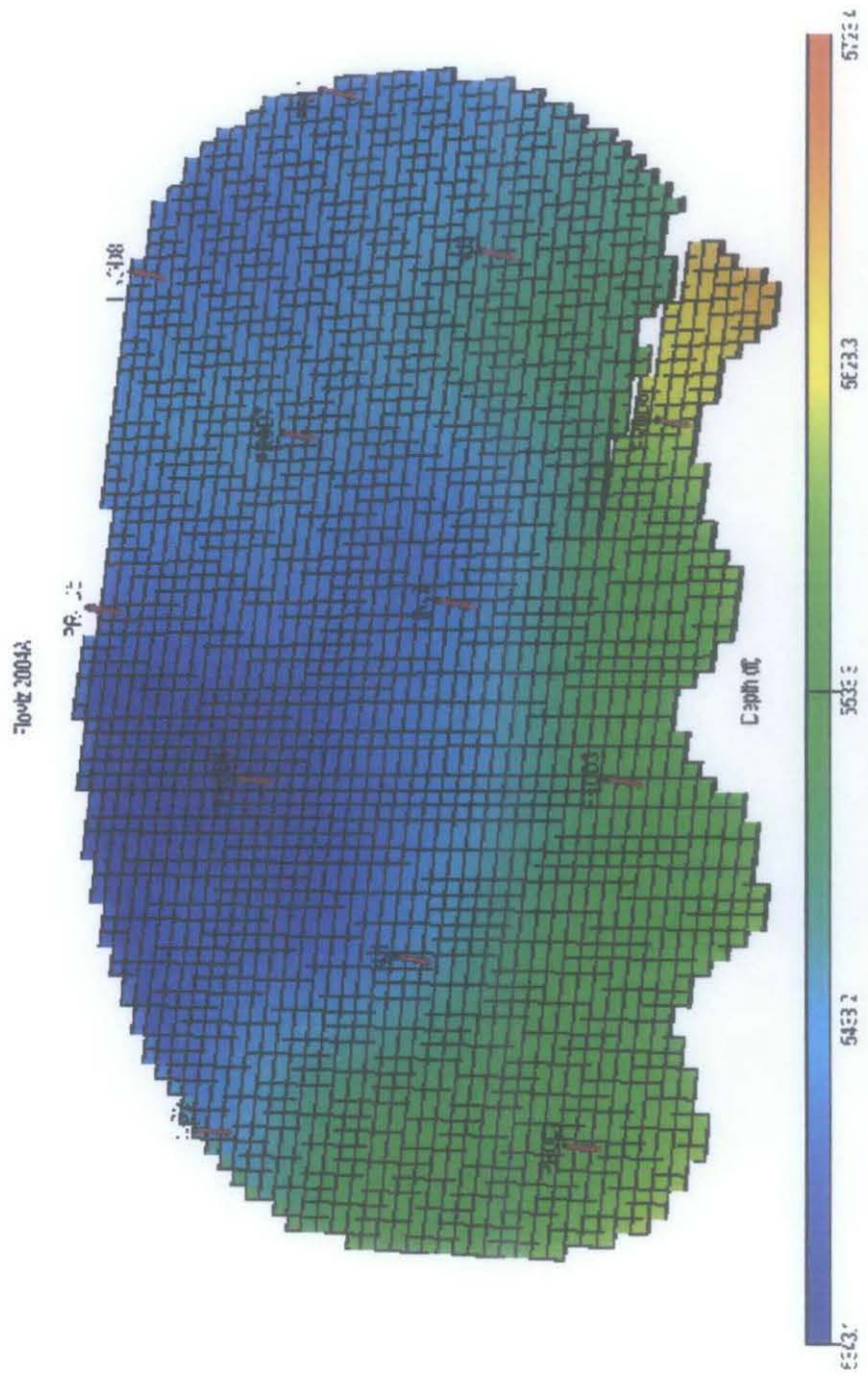
# WELLS ALLOCATION FOR CASE D (DIRECT LINE DRIVE) PATTERN
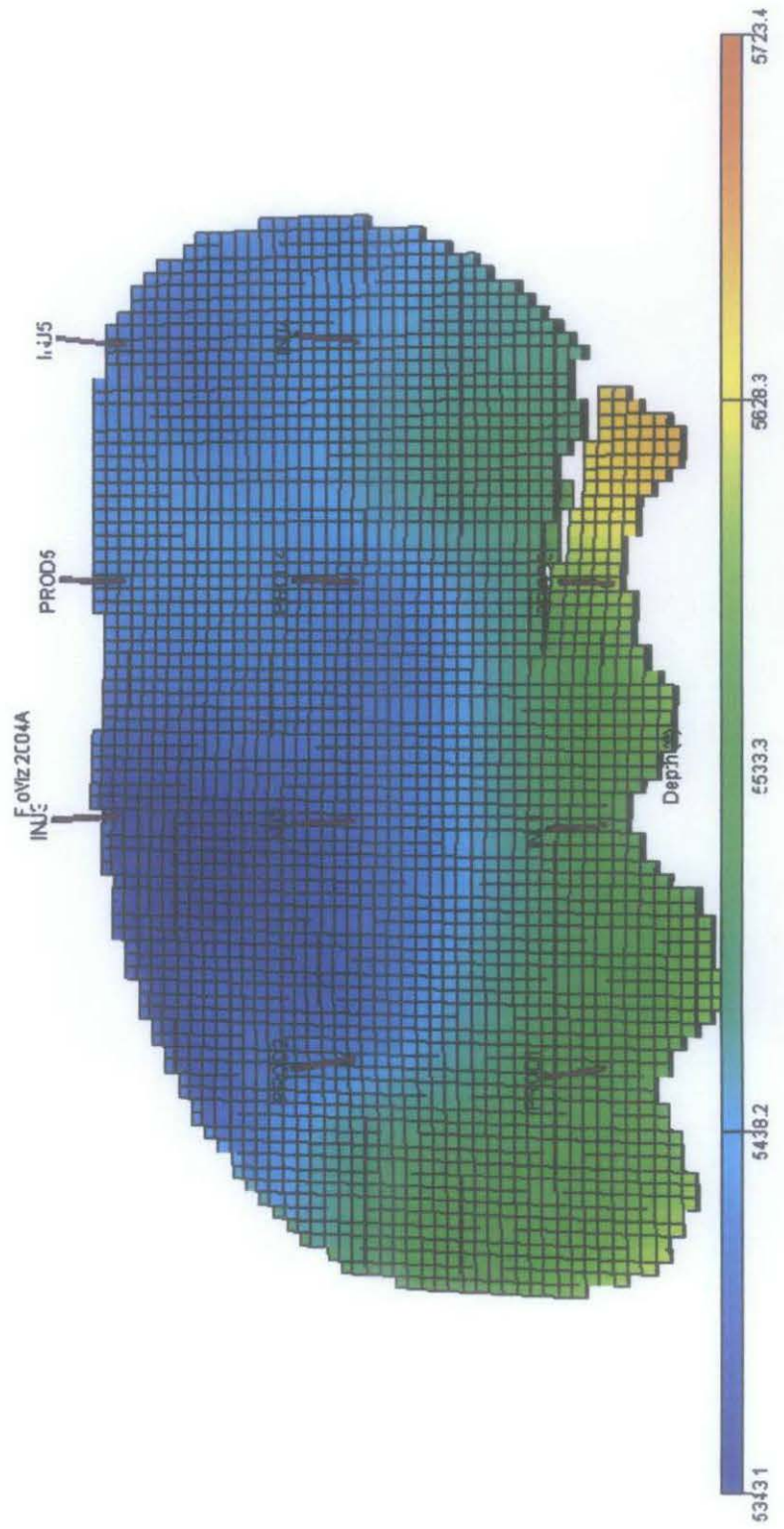
# WELLS ALLOCATION FOR CASE E (STAGGERED LINE DRIVE) PATTERN
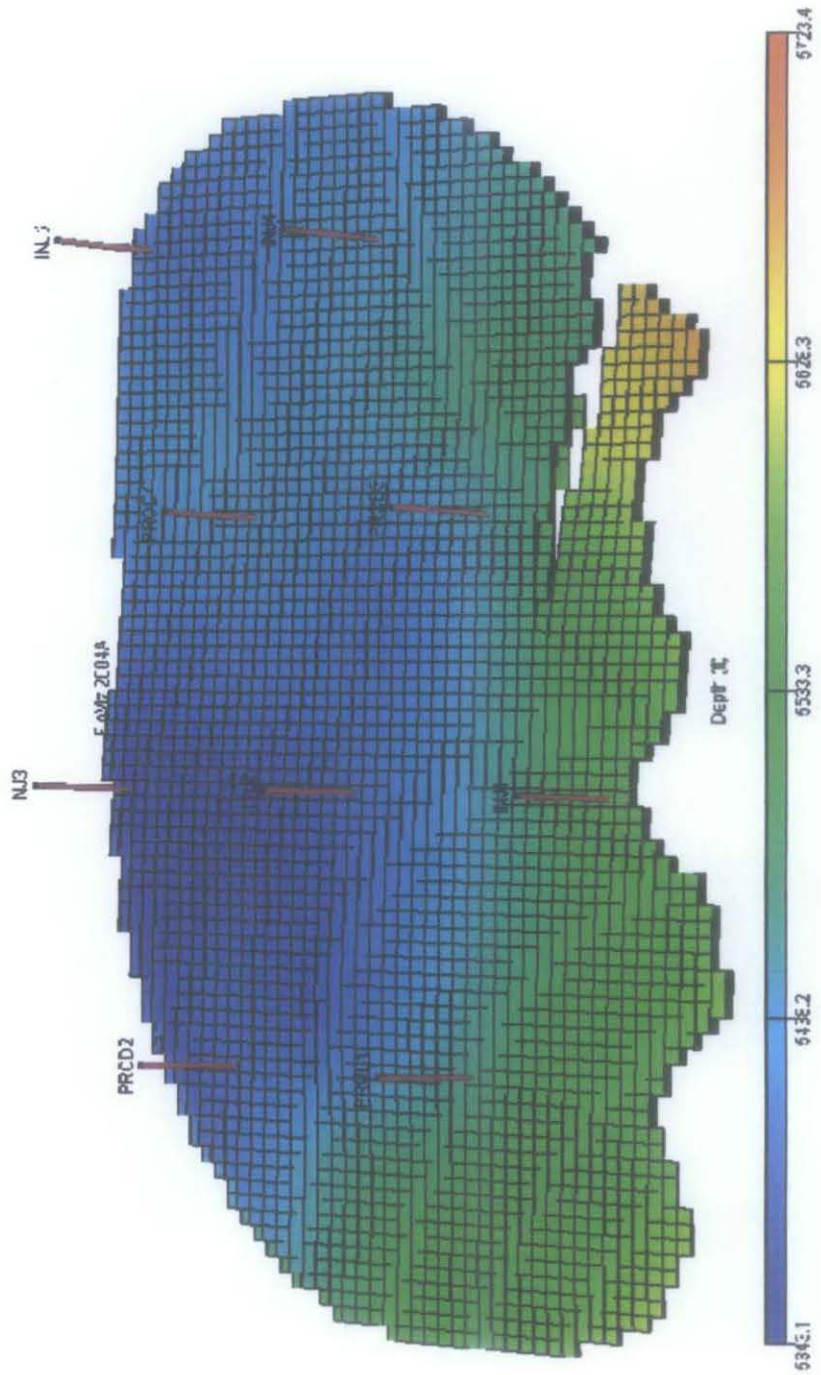
AREAL SWEEP EFFICIENCY FOR CASE A (FIVE SPOT) PATTERN
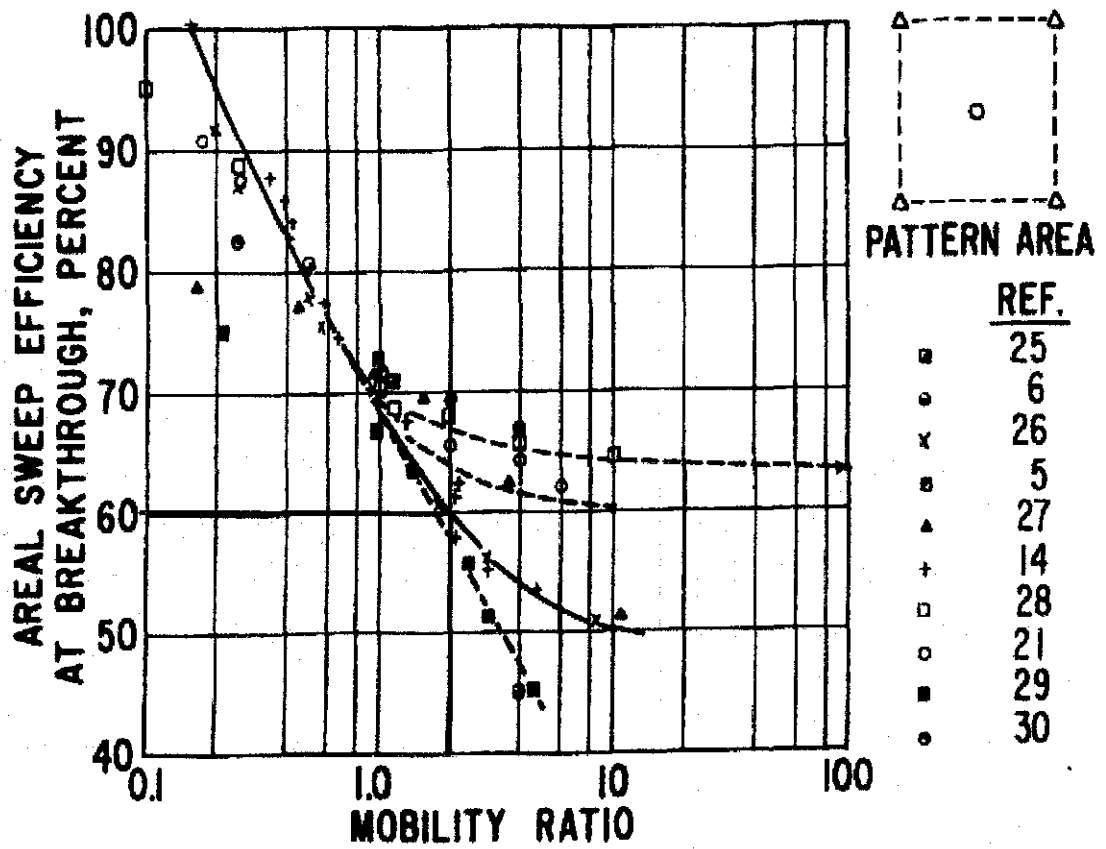


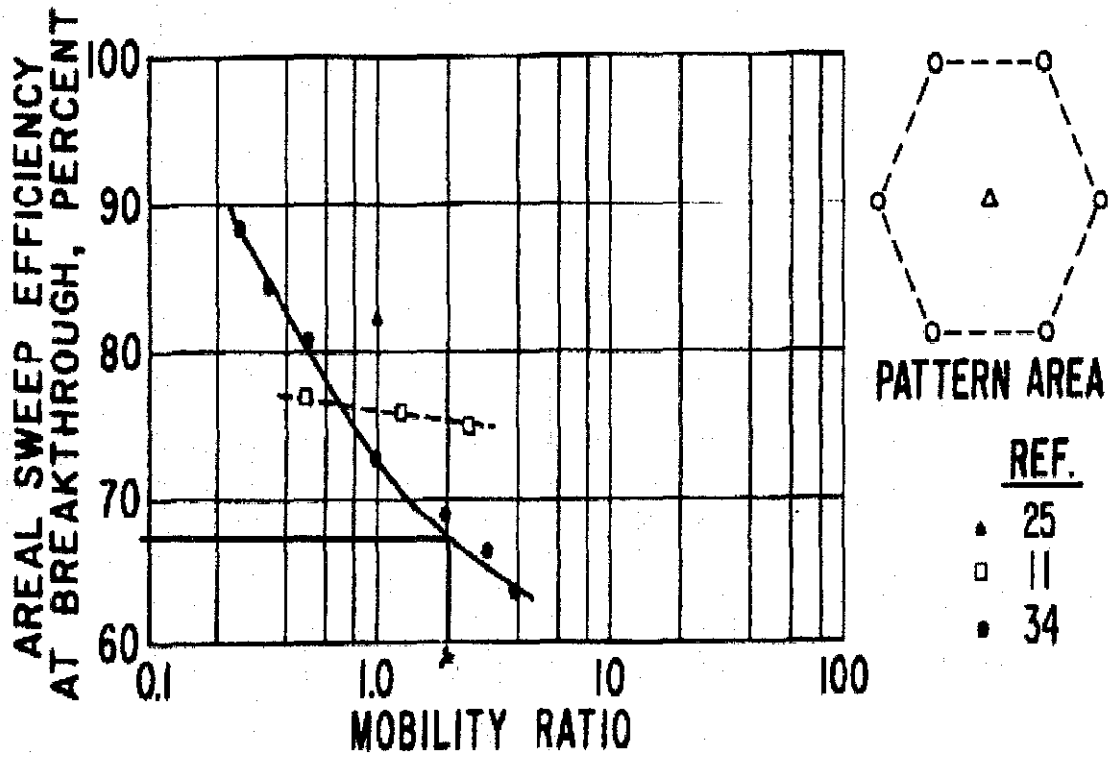Areal sweep efficiency at mobility ratio = 2.1 for developed five spot pattern (60%)

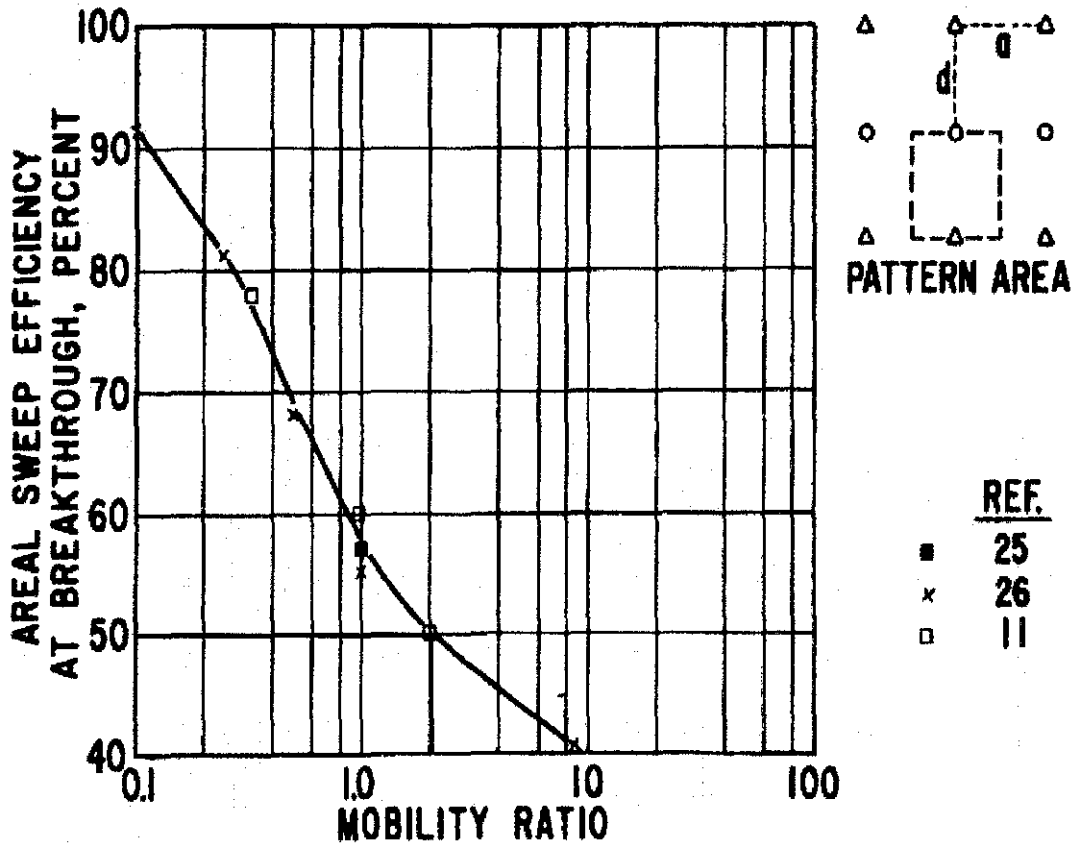# AREAL SWEEP EFFICIENCY FOR CASE B (SEVEN SPOT) PATTERN
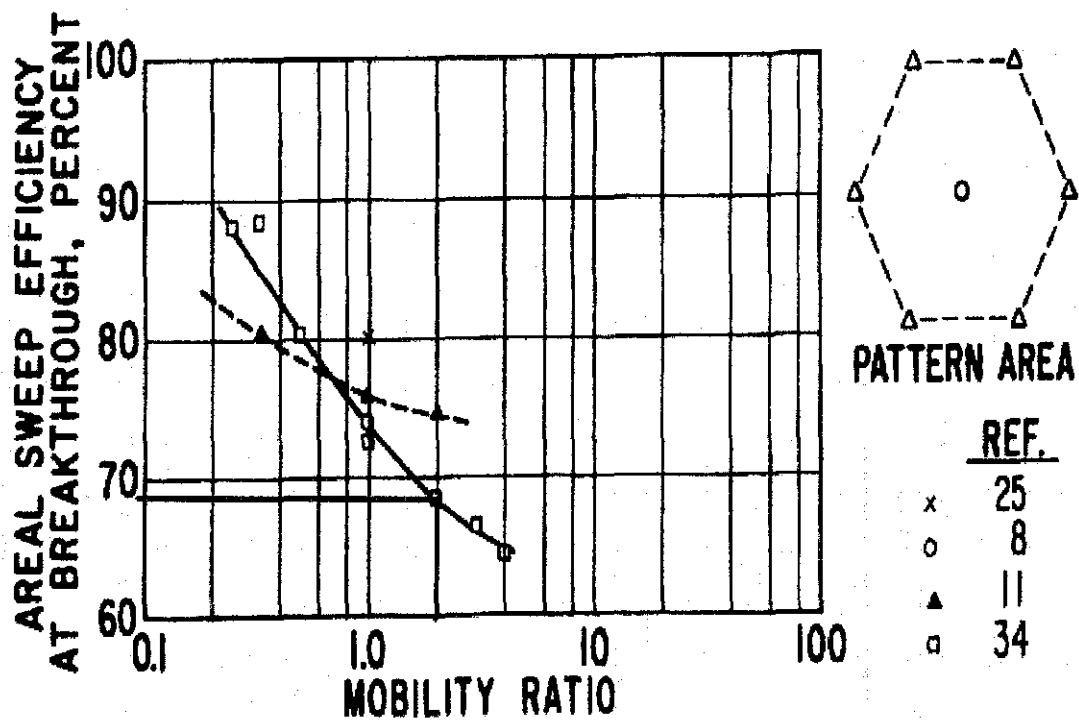


Areal sweep efficiency at mobility ratio = 2.1 for developed seven spot pattern (68%)

AREAL SWEEP EFFICIENCY FOR CASE C (INVERTED SEVEN SPOT)
PATTERN



Areal sweep efficiency at mobility ratio = 2.1 for developed inverted seven spot pattern

(66%)

AREAL SWEEP EFFICIENCY FOR CASE D (DIRECT LINE DRIVE) PATTERN



Areal sweep efficiency at mobility ratio = 2.1 for developed direct line drive pattern, d/a

= 1 (50%)

AREAL SWEEP EFFICIENCY FOR CASE E (STAGGERED LINE DRIVE)
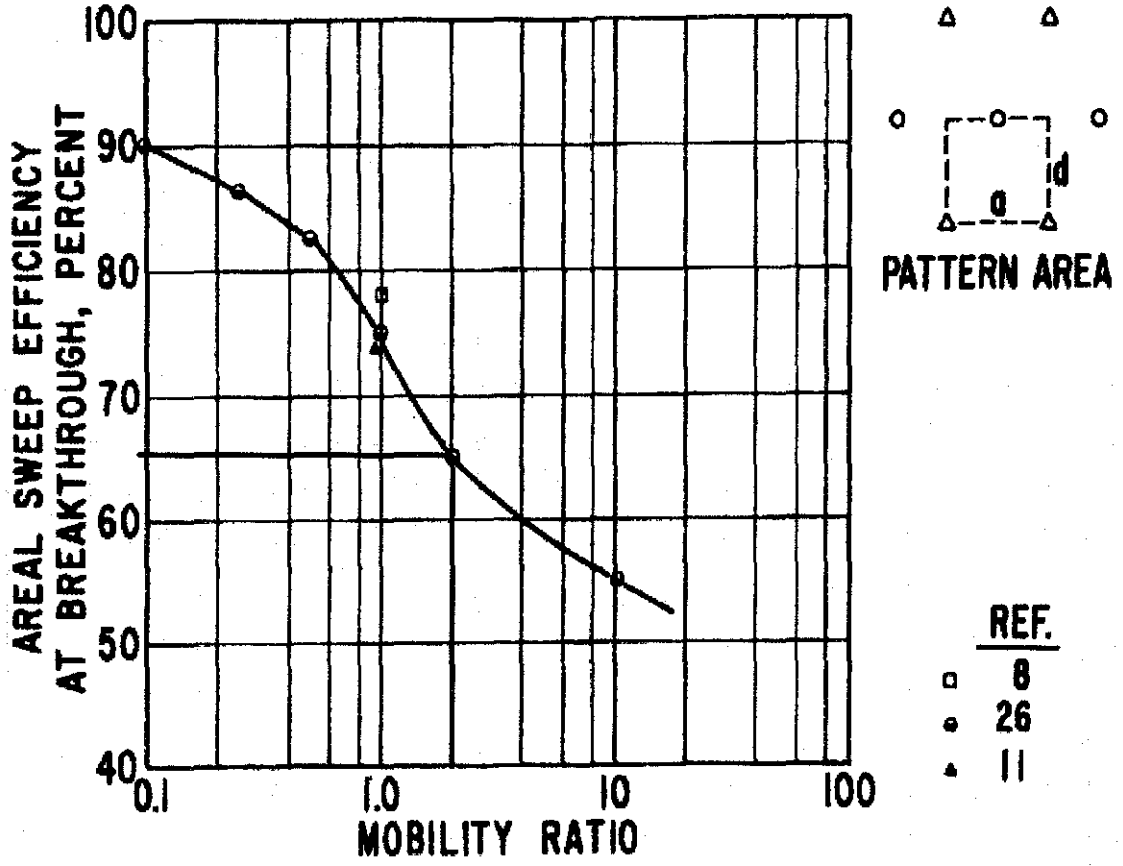
PATTERN



Areal sweep efficiency at mobility ratio = 2.1 for developed staggered line drive pattern,

d/a = 1 (65%)

## VALUE OF FRACTIONAL FLOW WITH RESPECT TO $CO_2$ SATURATION

| $CO_2$ saturation | Fractional flow, $f_s$ |
|---|---|
| 0.1 | 0.248233 |
| 0.2 | 0.426260 |
| 0.3 | 0.560174 |
| 0.4 | 0.664565 |
| 0.5 | 0.748225 |
| 0.6 | 0.816773 |
| 0.7 | 0.873963 |
| 0.8 | 0.922404 |
| 0.9 | 0.963959 |
| 1 | 1.000000 |

## CAPEX COSTS FOR ALL CASES OF WELL PATTERNS

| Structure | Price | Cases | | | | |
|---|---|---|---|---|---|---|
| | | Case A | Case B | Case C | Case D | Case E |
| Production well | USD4.86 million/unit | 24.31 | 14.59 | 43.76 | 24.31 | 19.45 |
| Injection well | USD6.69 million/unit | 53.48 | 60.17 | 20.06 | 33.43 | 33.43 |
| Total CAPEX, (USD million) | | 77.79 | 74.75 | 63.81 | 57.74 | 52.87 |
| CAPEX, (USD million + 30% contingencies) | | 101.13 | 97.18 | 82.96 | 75.06 | 68.74 |
| CUMULATIVE CAPEX, (USD million + 30% contingencies + 5% inflation) | | 105.02 | 100.92 | 86.15 | 77.95 | 71.38 |

## OPEX COSTS FOR ALL CASES OF WELL PATTERNS

| Structure | Based on CAPEX with 30% contingencies | Cases | | | | |
|---|---|---|---|---|---|---|
| | | Case A | Case B | Case C | Case D | Case E |
| Compressors | 9% | 9.10 | 8.75 | 7.47 | 6.76 | 6.19 |
| Structures / Jackets | 1% | 1.01 | 0.97 | 0.83 | 0.75 | 0.69 |
| Pipelines | 1% | 1.01 | 0.97 | 0.83 | 0.75 | 0.69 |
| Wells tangibles | 1% | 1.01 | 0.97 | 0.83 | 0.75 | 0.69 |
| On-shore terminals | 10% | 10.11 | 9.72 | 8.30 | 7.51 | 6.87 |
| Wells | USD0.5 million/well | 6.50 | 6.00 | 6.00 | 5.00 | 4.50 |
| TOTAL OPEX (USD million) | | 28.75 | 27.38 | 24.25 | 21.51 | 19.62 |
| CUMULATIVE OPEX AFTER 30 YEARS OF PRODUCTION (USD million) | | 862.46 | 821.39 | 727.52 | 645.38 | 588.66 |

## CALCULATION OF UNIT TECHNICAL COST FOR ALL CASES OF WELL PATTERNS

| ITEM | UNIT | CASES | | | | |
|---|---|---|---|---|---|---|
| | | Case A | Case B | Case C | Case D | Case E |
| Cumulative CAPEX | USD million | 105.02 | 100.92 | 86.15 | 77.94 | 71.38 |
| Cumulative OPEX | USD million | 862.46 | 821.39 | 727.52 | 645.38 | 588.66 |
| Total cost (CUM. CAPEX + CUM. OPEX) | USD million | 967.48 | 922.30 | 813.67 | 723.32 | 660.04 |
| Oil recovery | million barrel | 212.20 | 191.93 | 198.53 | 171.47 | 186.37 |
| UNIT TECHNICAL COST (TC / OR) | USD/barrel | 4.559 | 4.806 | 4.099 | 4.218 | 3.542 |